

CD103 and CD39 coexpression identifies neoantigen-specific cytotoxic T cells in colorectal cancers with low mutation burden

Jitske van den Bulk ,¹ Manon van der Ploeg,¹ Marieke E IJsselsteijn,¹ Dina Ruano,¹ Ruud van der Breggen,¹ Rebekka Duhen,² Koen C M J Peeters,³ Arantza Fariña-Sarasqueta,¹ Els M E Verdegaaal ,⁴ Sjoerd H van der Burg,⁴ Thomas Duhen ,⁵ Noel F C C de Miranda ¹

To cite: van den Bulk J, van der Ploeg M, IJsselsteijn ME, et al. CD103 and CD39 coexpression identifies neoantigen-specific cytotoxic T cells in colorectal cancers with low mutation burden. *Journal for ImmunoTherapy of Cancer* 2023;11:e005887. doi:10.1136/jitc-2022-005887

► Additional supplemental material is published online only. To view, please visit the journal online (<http://dx.doi.org/10.1136/jitc-2022-005887>).

Accepted 13 January 2023



© Author(s) (or their employer(s)) 2023. Re-use permitted under CC BY-NC. No commercial re-use. See rights and permissions. Published by BMJ.

¹Department of Pathology, Leiden University Medical Center, Leiden, The Netherlands

²Basic Immunology Lab, Earle A Chiles Research Institute, Portland, Oregon, USA

³Department of Surgery, Leiden University Medical Center, Leiden, The Netherlands

⁴Department of Medical Oncology, Oncode Institute, Leiden University Medical Center, Leiden, The Netherlands

⁵Anti-Cancer Immune Response Lab, Earle A Chiles Research Institute, Portland, Oregon, USA

Correspondence to

Dr Noel F C C de Miranda;
N.F.de_Miranda@lumc.nl

ABSTRACT

Background Expression of CD103 and CD39 has been found to pinpoint tumor-reactive CD8⁺ T cells in a variety of solid cancers. We aimed to investigate whether these markers specifically identify neoantigen-specific T cells in colorectal cancers (CRCs) with low mutation burden.

Experimental design Whole-exome and RNA sequencing of 11 mismatch repair-proficient (MMR-proficient) CRCs and corresponding healthy tissues were performed to determine the presence of putative neoantigens. In parallel, tumor-infiltrating lymphocytes (TILs) were cultured from the tumor fragments and, in parallel, CD8⁺ T cells were flow-sorted from their respective tumor digests based on single or combined expression of CD103 and CD39. Each subset was expanded and subsequently interrogated for neoantigen-directed reactivity with synthetic peptides. Neoantigen-directed reactivity was determined by flow cytometric analyses of T cell activation markers and ELISA-based detection of IFN- γ and granzyme B release. Additionally, imaging mass cytometry was applied to investigate the localization of CD103⁺CD39⁺ cytotoxic T cells in tumors.

Results Neoantigen-directed reactivity was only encountered in bulk TIL populations and CD103⁺CD39⁺ (double positive, DP) CD8⁺ T cell subsets but never in double-negative or single-positive subsets. Neoantigen-reactivity detected in bulk TIL but not in DP CD8⁺ T cells could be attributed to CD4⁺ T cells. CD8⁺ T cells that were located in direct contact with cancer cells in tumor tissues were enriched for CD103 and CD39 expression.

Conclusion Coexpression of CD103 and CD39 is characteristic of neoantigen-specific CD8⁺ T cells in MMR-proficient CRCs with low mutation burden. The exploitation of these subsets in the context of adoptive T cell transfer or engineered T cell receptor therapies is a promising avenue to extend the benefits of immunotherapy to an increasing number of CRC patients.

BACKGROUND

Immune checkpoint blockade therapy is an effective treatment option for colorectal cancer (CRC) patients diagnosed with mismatch repair (MMR)-deficient tumors,

WHAT IS ALREADY KNOWN ON THIS TOPIC

⇒ Neoantigen-specific T cells infiltrate mismatch repair-proficient (MMR-proficient) colorectal cancers despite their low to moderate mutation burden. Their presence warrants the development of immunotherapeutic approaches that leverage their potential for the treatment of patients diagnosed with MMR-proficient colorectal cancers.

WHAT THIS STUDY ADDS

⇒ Coexpression of CD103 and CD39 on CD8⁺ T cells was found to be a feature of neoantigen-specific T cells and, therefore, codetection of these markers can be employed to enrich for neoantigen-specific cytotoxic T cells from bulk tumor-infiltrating T cell populations.

HOW THIS STUDY MIGHT AFFECT RESEARCH, PRACTICE OR POLICY

⇒ The discovery of cell surface markers that pinpoint neoantigen-specific CD8⁺ T cells enables the development of adoptive T cell transfer products with increased anti-tumor activity and can support the discovery and exploitation of relevant T cell receptors for engineered T cell therapies.

while advanced MMR-proficient CRCs are generally refractory to immunotherapy.^{1–4} These contrasting outcomes can, to a great extent, be attributed to the greater availability of somatically mutated antigens (neoantigens) in MMR-deficient CRCs.⁵ The latter only comprise up to 5% of all advanced CRCs, thereby explaining the current limited applicability of immune checkpoint blockade in advanced CRC. Nevertheless, T cell responses against neoantigens have been extensively reported in patients diagnosed with MMR-proficient CRCs^{6–9} and, importantly, a proportion of these cancers appears

sensitive to immune checkpoint blockade therapy in a neoadjuvant setting.³

Naturally occurring antitumor T cell responses have been identified in a plethora of cancer types including ones with low immunogenicity (eg, cholangiocarcinoma, ovarian, and breast cancer).^{8 10–14} A major unaddressed question in the field is how to optimally leverage naturally occurring anti-tumor T cell responses to expand the benefit of immunotherapy to additional cancer patients. Adoptive T cell transfer (ACT) where patient's autologous tumor-reactive T cells are isolated and expanded *in vitro* to generate a therapeutic product is a straightforward approach to exploit tumor-reactive T cells.^{15–17} Objective clinical responses have been observed in approximately 50% of melanoma patients on ACT treatment,^{17–19} and encouraging outcomes have also been obtained in other solid cancers.^{14 20 21} The generation of ACT products generally results from the uncontrolled expansion of polyclonal T cell populations where loss of tumor-reactive T cells can occur.²² This undesired outcome may be favored when tumor-reactive T cells display dysfunctional phenotypes and are outnumbered by rapidly proliferating, non-tumor-reactive T cells. As previous works have shown, the enrichment of T cell populations with anti-tumor reactivity in ACT products is an attractive path to improve their efficacy.^{11 23}

Several groups have proposed molecular surrogates that pinpoint T cells with anticancer reactivity, including PD-1, TIM-3, LAG-3, OX40, CD39, CD103 and CD137.^{24–33} Previously, we reported that combined expression of CD103 and CD39 identifies tumor-reactive T cells and separates those from T cells with other specificities (eg, viral antigens).³⁴ CD103, also known as integrin α E, can dimerise to for example, integrin β 7 and orchestrate intraepithelial residency of T cells by binding to E-cadherin on epithelial cells.³⁵ CD39 is an ATP ectonucleotidase that is upregulated on chronically stimulated T cells and, together with CD73, produces adenosine which creates an immunosuppressive milieu. The expression of CD39 on T cells may

pinpoint chronic antigen stimulation which is likely to occur in the tumor microenvironment.^{27 36 37} Combined, CD103 and CD39 might constitute ideal surrogates to pinpoint neoantigen-specific T cells.

We previously demonstrated the existence of double-positive (DP), CD103⁺ and CD39⁺, CD8⁺ T cells in tumor digests of MMR-proficient CRCs, but the enrichment of neoantigen-specific CD8⁺ T cells within this population has not yet been demonstrated.³⁴ Therefore, we investigated in this study whether neoantigen-reactivity is contained within DP CD8⁺ T cell subsets in MMR-proficient CRCs and whether their specific isolation increases the capacity to detect neoantigen-specific T cells in comparison to reactivity assays performed on bulk tumor-infiltrating lymphocyte (TIL) populations.

METHODS

Tumor characterization

The original tumor location, clinical stage and Human Leucocyte Antigen (HLA) class I expression in the tumor cells are summarized in **table 1**. Only one patient, NIC16, received neoadjuvant chemoradiotherapy to which no clinical response was observed. The HLA class I status of the tumors was determined through immunohistochemical detection of HLA class I molecules with the HCA2 (1:3200; Nordic MUbio, Susteren, The Netherlands) and HC10 (1:3200; Nordic MUbio) clones, and β 2-microglobulin (clone EPR21752-214; 1:4000; Abcam, Cambridge, UK), as described previously.³⁸ The MMR status of the tumors was determined in a diagnostic setting at the department of pathology of the LUMC.

Collection and culturing of patient material

Patients' peripheral blood samples were obtained prior to surgery. Peripheral blood mononuclear cells (PBMC) were isolated from the heparinized venous blood by Ficoll-Amidotrizoate (provided by the LUMC pharmacy) gradient centrifugation. Tumor and corresponding

Table 1 Tumor characteristics

Patient ID	Tumor location	TNM stage	HLA IHC	CMS class
NIC4	Colon ascendens	pT3N0M0	Positive	4
NIC5	Sigmoid	pT3N2M0	Positive	2
NIC7	Sigmoid	pT2N1M0	Weak	2
NIC16	Rectum	ypT2N0M0	Positive	2
NIC17	Sigmoid	pT1N1M0	Positive	2
NIC20	Splenic flexure	pT3N0M0	Positive	2
NIC22	Rectum	pT2N0M0	Positive	2
NIC25	Hepatic flexure	pT3N1bM0	Defect	4
NIC27	Rectum	pT2N0M0	Heterogeneous	2
NIC38	Colon ascendens	pT1N0M0	Positive	3
NIC39	Rectum	pT3N2bM1	Positive	3

CMS, consensus molecular subtype; IHC, immunohistochemistry; TNM, tumor node metastasis.

normal colorectal tissue samples were obtained following surgery under supervision of a pathologist. Part of the tumor materials was snap-frozen, the remaining was cut into small fragments. Some small fragments were digested to single cell suspensions using 1 mg/mL collagenase D (Roche, Basel, Switzerland) and 50 µg/mL DNase I (Roche) in IMDM medium (Lonza BioWhittaker, Breda, The Netherlands), supplemented with 2 mM Glutamax (Thermo Fisher Scientific, Waltham, Massachusetts, USA), 20% Fetal Bovine Serum (Sigma-Aldrich, Saint Louis, Missouri, USA), 1% penicillin/streptomycin (Thermo Fisher Scientific), 1% Fungizone (Thermo Fisher Scientific), 0.1% Ciprofloxacin (provided by the LUMC pharmacy), and 0.1% Gentamicin (Sigma-Aldrich). The fragments were incubated for 30 min at 37°C and mechanically dissociated on a gentle-MACS Dissociator (Miltenyi Biotec, Bergisch Gladbach, Germany) in gentleMACS C tubes (Miltenyi Biotec). The suspension was passed through a 70 µm strainer (Miltenyi Biotec) and the flow through was cryopreserved.

In addition, 6–12 small tumor fragments were directly placed in culture in a 24-well plate with medium (IMDM (Lonza BioWhittaker), supplemented with 7.5% heat-inactivated pooled human serum (Sanquin, Amsterdam, The Netherlands), 1% penicillin/streptomycin (Thermo Fisher Scientific), and rIL-2 (1000 IU/mL; Aldesleukin, Novartis, Basel, Switzerland) for the outgrowth of TIL. After 14–21 days of culture, the T cells were counted and cryopreserved. To increase the number of T cells available for neoantigen-reactivity assays, TIL were expanded using a rapid expansion protocol in media containing rIL-2 (3000 IU/mL), OKT3 (Miltenyi Biotec, 30 ng/mL), and irradiated (40 Gy) feeder cells (100–200-fold excess) for 4–5 days, after which the culture was continued while refreshing medium with rIL-2 (3000 IU/mL), three times a week until a total culturing period of 2 weeks. The proportion of CD4⁺ and CD8⁺ T cells in the final expansion product was assessed by flow cytometry (online supplemental table S1).

Sorting and expansion of CD8⁺ T cell subsets

CD8⁺ T cell fractions were sorted on a BD FACSAria II (BD Biosciences, Franklin Lakes, New Jersey, USA) from single cell tumor digests and cultured as described previously.³⁴ In short, cells were selected for flow cytometric cell sorting based on the phenotypic markers CD45⁺, CD4[−], CD8⁺, CD45RA[−], CCR7^{+/-}, CD39^{+/-} and CD103^{+/-}. Additionally, the markers CD69, CD127 and PD-1 were assessed for phenotypic analyses. CD8⁺ T cells were sorted based on the expression of CD39 and/or CD103 (double-negatives (DN), single-positives (SP), and DP) and each subset was cultured separately in RPMI-1640 (Gibco, Thermo Fisher Scientific), supplemented with 10 ng/mL IL-15 (BioLegend, San Diego, California, USA), 2 mM glutamine (Gibco, Thermo Fisher Scientific), 1% non-essential amino acids (Gibco, Thermo Fisher Scientific), 1% sodium pyruvate (Gibco, Thermo Fisher Scientific), penicillin (50 IU/mL) + streptomycin (50 µg/

mL; Gibco, Thermo Fisher Scientific) and 10% pooled human serum (in house). T cells were stimulated with 1 µg/mL PHA (Remel, Dartford, UK) in the presence of irradiated (50 Gy) allogeneic feeder cells (2*10⁵ cells/well) in a 96-well round-bottom plate. If necessary, cells were restimulated in order to yield enough cells for downstream analysis. Cells were cryopreserved for analyses at later stages, after a total culturing period of 2–3 weeks. The DP subset of NIC5 and NIC39 did not expand and could, therefore, not be inspected for their ability to recognize neoantigens.

Neoantigen detection and binding prediction

Genomic DNA was isolated from snap-frozen tumor and corresponding normal colorectal tissues in order to prepare sequencing libraries as described previously.⁶ In brief, the NEBNext Ultra Directional RNA Library Prep kit for Illumina (New England Biolabs) and the NEBNext rRNA depletion kit (New England Biolabs) were employed to generate RNA sequencing libraries which were sequenced at Macrogen (Seoul, South-Korea) or Novogene (Cambridge, United Kingdom). The NEBNext Ultra II DNA Library Prep kit for Illumina (New England Biolabs, Ipswich, Massachusetts, USA) and the IDT xGEN Exome target kit (Integrated DNA Technologies, Leuven, Belgium) were used for preparation of the exome libraries. All kits were used according to the manufacturer's instructions.

RNA sequencing reads were first aligned to the human reference genome (build hg38) using STAR (V.2.7.3a).³⁹ For exome sequencing, the obtained 150 bp paired-end reads were mapped against the human reference genome (hg38) using the Burrows-Wheeler Aligner 3 algorithm (BWA-MEM V.0.7.17) BWA-MEM.⁴⁰ Picard Tools was used to remove duplicate reads⁴¹ and the Genome Analysis Toolkit 7 (GATK V.3.8)⁴² for base quality calibration. Subsequently, variant calling was done using a combination of three software tools, muTect 2, varScan and Strelka.^{43–46} The resulting .vcf files were then combined into a single file using GATK CombineVariants.⁴² RNAseq read counts for each variable allele was added to the identified variant chromosomal positions using the bam-readcount tool.⁴⁷

Functional annotation of the variants was done using the Ensembl Variant Effect Predictor.⁴⁸ Variants annotated as protein-altering were further investigated if at least one read with the alternative allele was present in the RNAseq data. In order to exclude false positives, variants were visually inspected using Integrative Genomics Viewer (IGV, Broad Institute).^{49–51} The 25-mer peptide sequences were generated for all the identified variants considered to be true. In case of frameshifts and stop loss mutations, several peptide sequences were generated which overlapped for at least half of the sequence (online supplemental table S2).

T cell reactivity assay

For the T cell reactivity assays, Epstein-Barr virus-transformed lymphoblastoid B cell lines (EBV-LCL) were

used as antigen-presenting cells rather than monocyte-derived dendritic cells because of the limited availability of autologous PBMCs. Autologous PBMC were immortalized by incubation with supernatant of the marmoset B cell line containing infectious particles of EBV strain B95-8 for 1 hour at 37°C in culture medium (RPMI-1640 (Lonza BioWhittaker), supplemented with 5 µg/mL PHA (Thermo Fisher Scientific), 10% FCS, L-glutamine (4mM), 1% penicillin/streptomycin (Thermo Fisher Scientific). The EBV-LCL were cultured for at least 3 weeks while refreshing the medium twice a week and cryopreserved for later use.

Neoantigen-directed reactivity of the T cells was investigated by a coculture assay as described previously.⁶ In short, autologous EBV-LCL were irradiated (60 Gy) and cocultured overnight with 20 µg/mL synthetic long peptides (25 amino acids). For all the identified variants, 25-mer peptide sequences were synthesized (Cell and Chemical Biology department at the LUMC, or PepScan, Lelystad, The Netherlands). T cells were added to the EBV-LCL at a 1:2 ratio, that is, respectively 15,000 and 30,000 cells per well. As negative controls, unloaded EBV-LCL with or without DMSO corresponding to the peptide solution were used. *Staphylococcus aureus* enterotoxin B (SEB; 0.5 µg/mL; Sigma-Aldrich) and PMA/Ionomycin (P/I; 20 ng/mL and 1 µg/mL, respectively; Merck, Darmstadt, Germany) were used as positive controls.

T cell reactivity was determined by performing ELISA to detect IFN-γ and granzyme B (Mabtech, Stockholm, Sweden) in the co-culture supernatants. In addition, CD137 expression on CD8⁺ T cells and CD40L and OX40 expression on CD4⁺ T cells were measured by flow cytometry on an LSRII Fortessa (BD Biosciences) making use of an antibody panel including anti-CD3-Amcyan (SK7, 1:20, BD Biosciences), anti-CD4-PE-CF594 (RPA-T4, 1:50, BD Biosciences), anti-CD8-APC-Cy7 (SK1, 1:40, BD Biosciences), anti-CD45-PerCP-Cy5.5 (2D1, 1:20, BD Biosciences), anti-CD40L-PE (TRAP1, 1:10, BD Biosciences), anti-CD137-APC (4B4-1, 1:100, BD Biosciences) and anti-OX40-FITC (ACT35, 1:20, BioLegend) antibodies. If T cell reactivity was detected by two independent assays, the respective neoantigen was taken along for further validation using HPLC-purified wild-type and mutant peptide sequences.

In order to confirm whether reactivity derived from CD4⁺ or CD8⁺ T cells in TIL cultures, we analyzed intracellular IFN-γ expression following the reactivity assays. Expanded TIL were cocultured with the respective neoantigen-loaded EBV-LCLs, as described above, and 10 µg/mL brefeldin A was added to the medium after 1 hour of coculture. The next day, T cells were inspected for the presence of intracellular IFN-γ-BV421 (4S.B3, 1:20, Biolegend), in combination with CD4-PE-CF594 (RPA-T4, 1:50, BD Biosciences), CD8-FITC (SK1, 1:20, BD Biosciences) and an APC-Cy7 live-dead marker (1:20, Invitrogen, Carlsbad, California, USA). Six thousand cells per subset were measured on a LSRII Fortessa (BD Biosciences).

CD8⁺ T cell characterization by imaging mass cytometry

T cell infiltration was assessed on formalin-fixed paraffin-embedded tissue sections using a general immunophenotyping imaging mass cytometry panel as described previously.⁵² For this study, we focused on the detection of CD3, CD4, CD8, CD39 and CD103, from a total of 40 markers on 18 MMR-proficient CRC patients (online supplemental table S3). H&E stains performed on consecutive tumor tissue slides were used to determine regions of interest. The 1000×1000 µm tissue areas were ablated and acquired by the Hyperion mass cytometry system (Fluidigm, San Francisco, California, USA). The generated MCD files were exported and visualized with the Fluidigm MCD viewer to set signal threshold per marker in order to better separate antibody signal from noise.

Statistics

Paired samples Wilcoxon test was applied to test differential CD8⁺ T cell infiltration in epithelial and stromal tissue compartments in tumors, as determined by imaging mass cytometry. One-way analysis of variance was applied to test differences in the relative frequency of cell surface markers on the different T cell subsets. Statistical testing and graphical representation were performed with Graphpad Prism V.9.3.1.

Data availability

Additional data generated in this study are available on reasonable request to the corresponding author. RNAseq of the studied patients will be made available in the Sequence Read Archive of NCBI via PRJNA911749.

RESULTS

Neoantigen reactivity by cytotoxic T cells is contained within the CD103⁺CD39⁺ subset

In order to evaluate whether neoantigen reactivity is associated with CD103⁺ and CD39⁺ expression on CD8⁺ T cells, we evaluated T cell responses against synthetic peptides corresponding to neoantigens in bulk TIL and in CD103⁻CD39⁻ (DN), CD103⁺CD39⁻/CD103⁻CD39⁺ (SP), and CD103⁺CD39⁺ (DP) CD8⁺ T cell populations, isolated from single cell digests, derived from 11 MMR-proficient CRCs (figure 1A). All tumors retained β2-microglobulin expression and the majority of tumors were found to be proficient in HLA class I expression as determined by immunohistochemistry (table 1). Loss of HLA class I expression was observed in NIC25 while the tumor sample from NIC27 presented a heterogeneous pattern of HLA class I expression.

The proportion of CD103 and/or CD39-positive CD8⁺ T cell subsets was generally low among the total immune cell populations (CD45⁺ cells) (online supplemental figure S1A). Furthermore, the relative frequencies of the flow sorted CD8⁺ T cell populations (DP, SP and DN) were highly variable between patients (online supplemental figure S1B). In particular, SP CD8⁺ T cells with CD39 expression were rare in this cohort which hampered

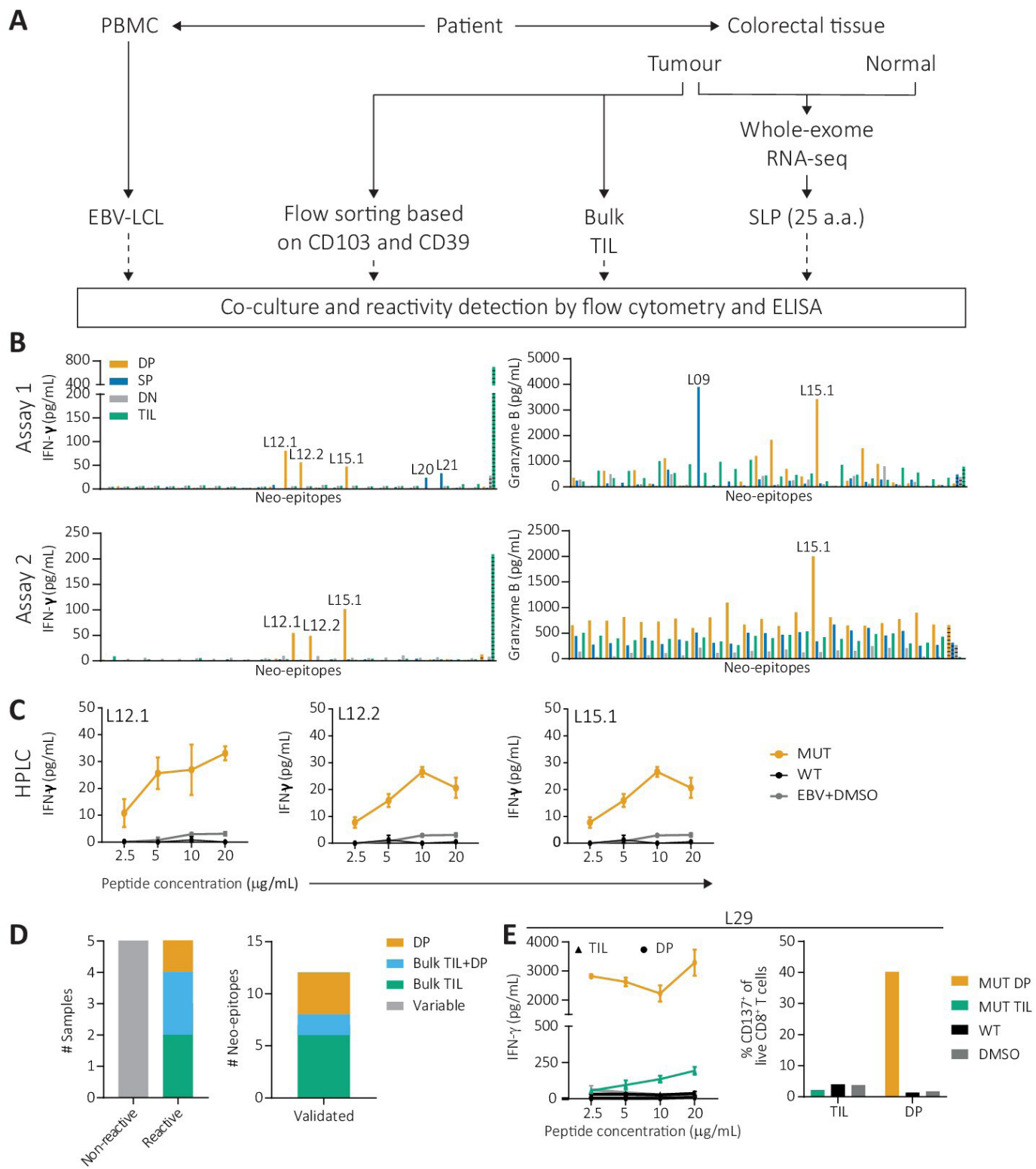


Figure 1 Neoantigen-directed T cell reactivity assessment from bulk TIL and sorted CD8⁺ T cell subsets according to CD33 and CD103 expression. (A) Schematic workflow of the experimental setup. (B) A representative example of the IFN- γ and granzyme B ELISA measurements obtained in two independent assays performed in NIC16. Potential neoepitopes are depicted with the peptide number, for example, 'L12.1'. (C) Representative example of a validation experiment in NIC16. The differential IFN- γ production upon coculture with the mutant peptide (yellow), the corresponding wild-type peptide (black) or a DMSO control (grey) was assessed in a peptide titration series ranging from 2.5 to 20 μ g/mL. (D) Summary of the number of patient samples in which no reactivity was detected (gray), or with T cell responses derived from the DP subset (yellow), bulk TIL (green) or both the bulk TIL and DP subset (light blue). (E) IFN- γ production (left) and CD137 expression (right) on coculture of NIC4 bulk TIL (green) and DP subset (yellow) with the L29 epitope and controls. DP, double-positive; EBV-LCL, Epstein-Barr virus-transformed lymphoblastoid B cell lines; PBMC, peripheral blood mononuclear cell; TIL, tumor-infiltrating lymphocyte.

their specific expansion. NIC5 formed an exception as both CD103⁻CD39⁺ and CD103⁺CD39⁻ subsets could be separately expanded and taken along for neoantigen reactivity assays. The number of sorted cells varied from 18 to 31 000 cells per subset, with a median of 595 cells (online supplemental table S4). Most CD8⁺ T cell subsets expanded more than 2000 times (median of 17973 times) after culture, with the exception of two samples (NIC5 DP and NIC39 DP) which did not expand. Of note, the DN subset expanded at a higher rate than the subsets expressing CD39 and/or CD103 (online supplemental table S4). Also, preferential expansion of CD4⁺ T cells over CD8⁺ T cells was observed in the expanded bulk TIL samples (online supplemental table S1). Phenotypic analyses of the CD8⁺ T cells subsets revealed that CD69 and PD-1 (traditional activation markers) expression were most frequent in the DP subset and less abundant in DN CD8⁺ T cells, in contrast to CD127 (IL-7R) expression which was found to be enriched in DN CD8⁺ T cells (online supplemental figure S1C-F).

Whole-exome and transcriptome sequencing were performed on cancer and healthy tissues for the identification of putative neoantigens. All CRCs presented a low number of non-synonymous mutations, with a median of 38 transcribed mutations (21–57, **table 2**). All expressed, non-synonymous mutations were considered potential neoantigens. T cell reactivity was assessed by measuring the capacity of T cells to secrete IFN-γ and granzyme B (measured by ELISA) and to upregulate activation markers (measured by flow cytometry) after coculture with autologous EBV-LCL, loaded with mutated synthetic long peptides (25AA). The DN subset produced widespread, unspecific reactivity in the majority (n=6) of samples, which is likely explained by the presence of EBV-specific T cells in this population. Mutated peptides that consistently induced the secretion of IFN-γ and/or granzyme B by T cells, in two independent replicate coculture assays, were considered as potential immunogenic neoantigens (**figure 1B**, online supplemental figure S2). For example, in patient NIC16, the peptides L12.1, L12.2 and L15.1 were identified as potential epitopes, while L09, L20 and L21 were not pursued further they only induced reactivity in one of the assays (**figure 1B**). Reactivities were confirmed by coculture with the mutant and the corresponding wild-type HPLC-purified peptides. Release of IFN-γ or granzyme B, or CD137 upregulation on CD8⁺ T cells with the mutant peptide and not the corresponding wild type was considered as a bona fide neoantigen-specific T cell response (**figure 1C**).

Neoantigen-specific T cell responses were validated in five patients (NIC4, NIC16, NIC20, NIC22, and NIC38), against 1–3 neoantigens per patient (**figure 1D, table 2**). The tumors of these patients were all found to have retained HLA class I expression on the surface of cancer cells, while two of the samples with no detectable neoantigen-reactivity displayed

abnormal HLA class I expression which could possibly interfere with the persistence of neoantigen-reactive CD8⁺ T cells in the tissue. Interestingly, in these two patients the DP CD8⁺ T cell subsets were also found to display suboptimal characteristics as the DP CD8⁺ T cells of NIC25 were PD-1⁺CD39^{low} and half of the DP CD8⁺ T cells of NIC7 were PD-1⁺CD127⁺. These phenotypes suggest the absence (NIC25) or low abundance (NIC7) of properly activated CD8⁺ T cells. Reactivity could only be detected in either the DP CD8⁺ T cell subset or in the bulk TIL samples. None of the SP or DN subsets displayed neoantigen-specific T cell responses.

In **figure 1C**, representative assays are shown corresponding to the detection of neoantigen-specific reactivity in the DP CD8⁺ T cell subset against two epitopes representing the *ENGASE* c.260T>G (p.C87W, peptide L12.1 and L12.2) and *SMPD4* c.646G>T (p.V216F, peptide L15.1) mutations. No reactivity for this patient could be detected in the bulk TIL. The DP CD8⁺ T cell subset of NIC20 recognized two peptides corresponding to the *MYOBI* c.801A>C (p.E267D, peptide L16.2) and *KMT2C* c.8950dupA (p.S2984fs, peptide L27.2) mutations (online supplemental figure S3). Of note, cross-reactivity was also detected to the wild-type peptides of NIC20. The bulk TIL of NIC20 recognized the same peptide derived from the *MYOBI* mutation but not the one derived from *KMT2C*. In NIC4, reactivity against the mutation *PDP1* c.1024C>T (p.R342W, peptide L29) was detected in both DP CD8⁺ and TIL samples.⁶

Neoantigen reactivity in bulk TIL samples—without concurrent reactivity of the DP CD8⁺ T cell subset—was detected in NIC4, NIC22 and NIC38. For NIC22, bulk TIL recognized the peptides corresponding to the mutations *RRP15* c.187A>G (p.I63V, peptide L02) and *CHEK2* c.1418C>G (p.A473G, peptide L20; **table 2**). In NIC38, bulk TIL reactivity was detected to the epitopes from the following mutations: *RALGAPB* c.3410C>T (p.A1137V, peptide L36), *GNAS* c.557G>A (p.R186H, peptide L37) and *SHH* c.962G>A (p.R321H, peptide L48). In addition to the *PDP1* mutation that was recognized by both DP CD8⁺ T cell and bulk TIL, two peptides showed reactivity only in the bulk TIL from NIC4 (*ACTR10* p.R213H, peptide L06; *RAE1* p.X369W, peptide L20).

In total, T cell responses were identified against 12 unique neoepitopes; 4 neoepitopes were recognized by the DP CD8⁺ T cell subsets, 2 neoepitopes were detected by both the DP CD8⁺ T cells and bulk TIL and, lastly, 6 neoepitopes were recognized only by the bulk TIL (**figure 1D**). Since a considerable number of neoepitopes were only recognized by the bulk TIL samples, we hypothesized that recognition of those epitopes could be mediated by CD4⁺ T cells. Flow cytometry analyses revealed that all reactivity detected exclusively in bulk TIL samples was derived from CD4⁺ T cells as determined by OX40 and/or intracellular IFN-γ upregulation following coculture with peptides (**figure 1**

Table 2 Patient's neo-epitopes to which T cell reactivity was detected

Patient ID	CMS	# Mut	# SLP	Genes	Mut cDNA	Mut aa.	Peptide	Peptide ID	Reactive T cell product	CD4/8
NIC4	4	30	39	ACTR10	c.638G>A	p.R213H	SVPEGVLEDIKAHTCFVSDLKRGKX	L06	TIL	CD4
				RAE1	c.1106A>G	p.X369W	WMILETTLAQPFLISTPLHLCTNLGP	L20	TIL	CD4
				PDP1	c.1024C>T	p.F342W	PKSEAKSVVKQDMLGLMPFRAFG	L29	TIL, DP	CD8
NIC5	2	56	71	—	—	—	—	—	—	—
NIC7	2	33	44	—	—	—	—	—	—	—
NIC16	2	21	23	ENGASE	c.260T>G	p.C87W	PPLSSQRPRRTLWHDMMGGYLDDRF	L12.1	DP	CD4
				ENGASE	c.260T>G	p.C87W	RNAMQIVEMDHDSESVLAVWMAA	L12.2	DP	CD8
NIC17	2	43	47	—	—	—	—	—	—	—
NIC20	2	30	34	MYOBI	c.801A>C	p.E267D	RPLSSQRPRRTLWHDMMGGYLDDRF	L12.1	DP	CD4
NIC22	2	30	34	RRP15	c.895D>A	p.S2984fs	NVTWSRWNHVFESCAAGKRABRSRSINS	L27.2	DP	CD4
NIC38	3	54	75	RALGAPB	c.3410C>T	p.A1137V	EPANSRLPFPHLVLDSTIGFFDOI	L36	TIL	CD4
NIC25	4	38	47	—	—	—	—	—	—	—
NIC27	2	26	43	—	—	—	—	—	—	—
NIC39	3	57	66	SHH	c.557G>A	p.R186H	DYVPSDQDLIRCHMITSGEETKFO	L37	TIL	CD4
				GNA3	c.557G>A	p.R186H	VADGQRYVVAWEHDODRLLPAWH	L48	TIL	CD4
										—

aa, amino acid; CMS, consensus molecular subtypes; DP, double-positive; Mu, mutation; SLP, synthetic long peptide.

(NIC16; online supplemental figure S3 (NIC38); online supplemental figure S4 (NIC4, NIC22)).

In sum, CD8⁺ T cell reactivity in MMR-proficient CRC is largely contained within the DP subset and, importantly, the specific interrogation of this population allowed the discovery of neoantigen-specific reactivity that could not be detected in bulk TIL samples. In line with this, the higher levels of IFN- γ production and CD137 expressing cells upon peptide stimulation reflects a higher frequency of neoantigen-specific cells in the DP CD8⁺ subset than in the bulk TIL sample (figure 1E).

CD103⁺CD39⁺ CD8⁺ T cell subsets are enriched in the epithelial compartment of CRC

To interrogate the distribution of the different CD8⁺ T cell subsets in the tumor microenvironment of CRC, we applied imaging mass cytometry on 18 CRC tissues, including the 11 samples for which neoantigen reactivity was investigated (figure 2A,B). The relative frequency of the DP cells, in relation to the total number of CD8⁺ T cells, was significantly higher (5.7x) in the epithelial compartment of tumor tissues than in the stromal areas (figure 2C, paired samples Wilcoxon test: p=0.002). In the tumor stroma, CD8⁺ T cells often lacked the coexpression of these markers (figure 2B) while the majority of intraepithelial CD8⁺ T cells expressed CD103 and CD39 (figure 2A). This observation suggests a direct interaction between the DP CD8⁺ T cells and cancer cells, therefore, supporting their important role in cancer immunity.

DISCUSSION

Innovative treatment options are required for patients diagnosed with advanced CRC. Since we and others identified the presence of neoantigen-specific T cells in MMR-proficient CRC patients, there is a realistic expectation that T-cell based immunotherapy can also be successful in this patient group.^{6–9} Furthermore, the majority of MMR-proficient colorectal tumors are found to retain HLA class I expression,³⁸ indicating that they remain susceptible to CD8⁺ T cell-mediated tumor eradication. Their general refractoriness to immune checkpoint blockade treatment in the advanced setting might be explained by the low frequency of neoantigen-specific T cells in tissues but also a dominant immunosuppressive microenvironment like the one provided by TGF- β activation in a substantial proportion of MMR-proficient CRC.^{6,53,54}

An attractive path worth exploring for the treatment of cancers with low immunogenicity is the development of ACT protocols that specifically focus on neoantigen-specific T cells. To achieve optimal ACT treatments for those patients, the definition of cellular biomarkers that can be used as surrogates of neoantigen-specificity but also be targeted in cell sorting procedures is paramount.

Previously, CD103 expression on cytotoxic T cells was highlighted as a prognostic marker for breast and ovarian cancer patient survival,^{24,55,56} and associated to positive treatment outcomes in lung and bladder cancer patients who received anti-PD-L1 therapy, intratumorally.⁵⁷ Also, loss of the CD103 ligand, E-cadherin, was found to reduce the response to checkpoint blockade therapy in murine melanoma.⁵⁸ Combined expression of CD103 and CD39 has been reported to pinpoint tumor-reactive CD8⁺ T cells in melanoma and head and neck cancer.^{9,27,34} DP CD8⁺ T cells were more frequently positive for CD69 and negative for CD127 and expressed higher levels of PD-1. Together, this cell surface expression pattern supports a chronic activation phenotype in the DP CD8⁺ T cell subset.³⁶ On the other hand, the expression of these markers did not provide enough specificity to define neoantigen-reactive T cells as compared with the codetection of CD103 and CD39.

CD103⁺CD39⁺ CD8⁺ T cells were previously found to be clonally expanded in tumor tissues and to present enhanced granzyme B expression in comparison to other CD8⁺ T cell subsets.^{27,34} In line with these findings, we show that CD8⁺ T cell-derived neoantigen reactivity is limited to populations expressing CD103 and CD39. The relevance of DP CD8⁺ T cells in the antitumor response is highlighted by the fact that their frequency within the tumor epithelium was significantly higher than in the stromal compartment, supporting the occurrence of physical interactions between this subset and cancer cells. In our study, 1–3 neoepitopes eliciting T cell reactivity were identified, per patient, which translates to a neoantigen detection rate of 2.6% in relation to the total number of expressed mutations. Importantly, the interrogation of neoantigen reactivity in the DP CD8⁺ T cell subsets led to the identification of additional epitopes recognized by CD8⁺ T cells as compared with bulk TIL. Furthermore, we observed that DN CD8⁺ T cells expanded at a higher rate than SP and DP CD8⁺ T cells, suggesting that the latter subsets may be under-represented in expanded bulk TIL populations. Furthermore, we also observed that bulk TIL products were, in general, enriched for CD4⁺ T cells, again, affecting the probability that neoantigen-reactive CD8⁺ T cells are contained within unselected T cell products. Altogether, our observations highlight the possibility of undertaking immunotherapeutic strategies in MMR-proficient CRC patients through the enrichment of CD103⁺CD39⁺ neoantigen-specific CD8⁺ T cells for the development of therapeutic T cell products. In parallel, it would be important to investigate whether clinical responses to immune checkpoint blockade therapies in MMR-proficient CRC³ are related to the frequency of DP CD8⁺ T cells. Interestingly, PD-1 expression on its own did not appear to be an ideal biomarker to pinpoint neoantigen-specific T cells in this cohort (online supplemental figure S1).

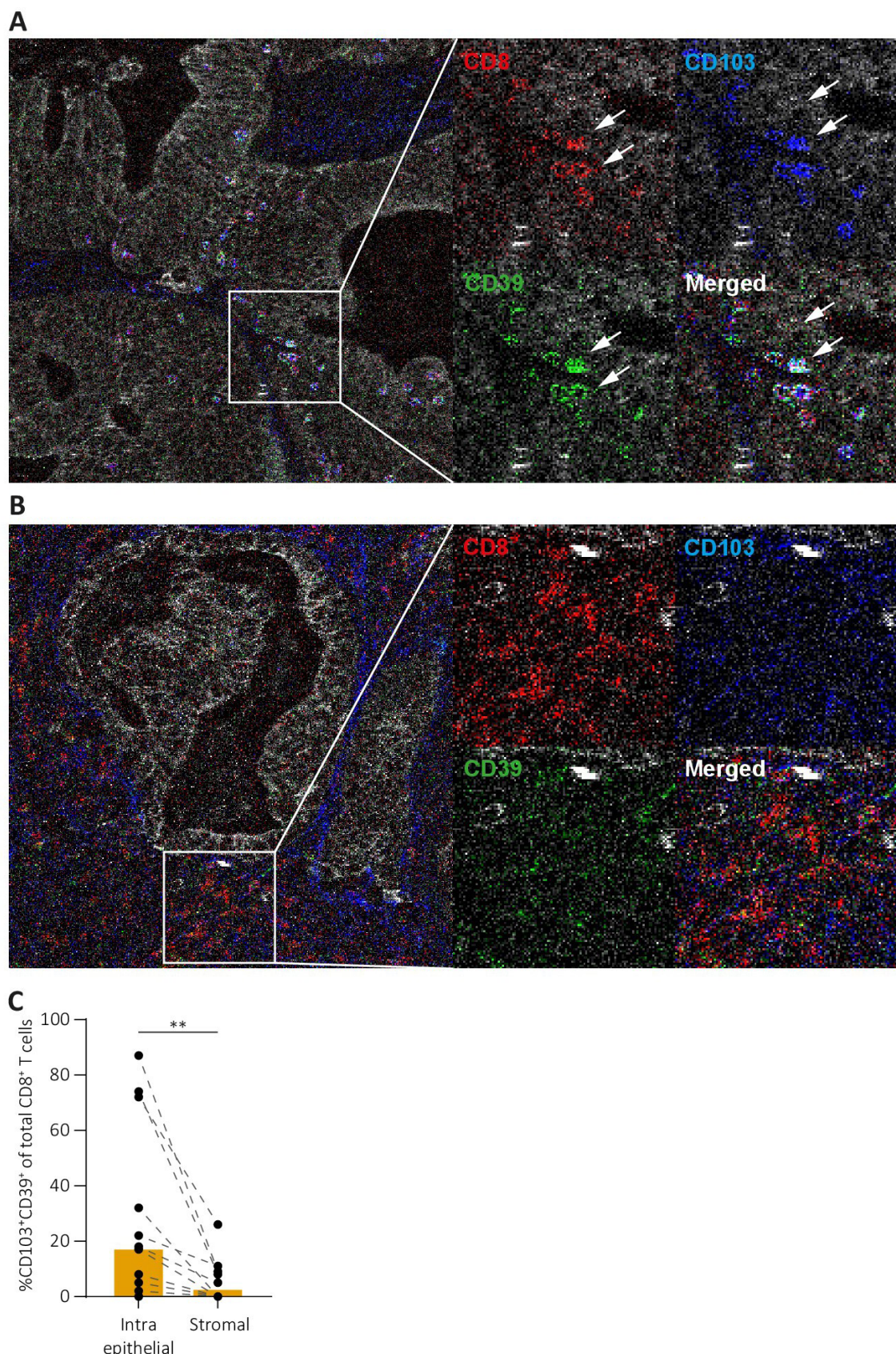


Figure 2 CD103 and CD39 detection on tumor-infiltrating T cells using imaging mass cytometry. (A, B) Representative tissue sections illustrating T cell infiltration (CD8 in red, CD103 in blue, CD39 in green) in relation to cancer cells (keratin, white). The arrows highlight DP CD8⁺ T cells. (C) Quantification of infiltration by DP populations as percentage of the total CD8⁺ T cell infiltrate. The number of cells was measured for the epithelium and stroma separately, and compared between both compartments using a paired samples Wilcoxon test. **, P ≤ 0.01. DP, double-positive.

Whether CD39 expression translates to an ‘exhausted’ or ‘dysfunctional’ T cell state that would compromise the exploitation of DP CD8⁺ T cells for ACT, remains a point of discussion.^{34 37 59} In the first days after activation of naïve T cells, transient CD39 expression takes place but, CD39—together with other coinhibitory molecules—can also be expressed by T cells after chronic antigen stimulation in the tumor microenvironment.⁶⁰ Nevertheless, we were able to expand DP CD8⁺ T cells *in vitro* (median=7419 times) and their successful application in neoantigen reactivity assays demonstrates that this subset retains functional activity. Further studies should be performed to examine whether DP CD8⁺ T cells still harbor functional cytotoxic capacity *in vivo*. Alternatively, the isolation of DP CD8⁺ T cells could instead be employed for the identification of neoantigen-specific T cell receptors (TCRs) that can then be engineered into donor T cells with optimal functionality. Such an approach has recently been reported for the treatment of a patient with metastatic pancreatic cancer harboring the KRAS^{G12D} mutation and expressing HLA-C*08:02.⁶¹ Specifically, the authors genetically engineered the patient’s T cells to express two TCRs, previously identified in a metastatic CRC patient, with that specific restriction. The infused ACT product led to regression of the metastases, which was still ongoing 6months postinfusion. This case study illustrates the safety, feasibility and wide applicability of using previously identified TCRs in ACT treatments.

In addition to CD8⁺ T cell-mediated responses, we observed CD4⁺ T cell reactivity among the bulk TIL in several patients. This observation is in line with previous reports on MMR-proficient CRC where approximately half of the T cell reactivity was attributed to CD4⁺ T cells.⁶⁻⁸ Importantly, ACT approaches making use of neoantigen-specific CD4⁺ T cells were shown to be successful, supporting the relevance of including CD4⁺ T cells in ACT products for optimal tumor eradication.^{11 17} However, little is yet known about cell surface markers that specifically pinpoint tumor-reactive T cell subsets among CD4⁺ T cells. A recent study proposed that CD39 can guide the enrichment of tumor-reactive CD4⁺ T cells.^{30 62} Single cell transcriptomic data from head and neck, cervical and ovarian cancer samples revealed similar transcriptional programs between PD-1^{hi}CD39⁺ CD4⁺ T cells and neoantigen-specific CD8⁺ T cell subsets,^{32 63} for example, *TOX* and *CXCL13* expression. However, as these markers are not expressed at the cell surface they cannot be employed for the specific isolation of neoantigen-specific CD4⁺ T cells. Alternatively, combined expression of PD-1 and ICOS has been proposed to identify populations of neoantigen and tumor-associated antigen-specific CD4⁺ T cells.⁶⁴ The limited availability of patient material in this cohort did not allow us to explore this question in more detail leaving this topic open for future investigations.

In conclusion, we report here that in MMR-proficient CRC patients neoantigen-directed CD8⁺ T cell reactivity is mainly contained in the CD103⁺CD39⁺ subset. Their isolation can be exploited to enrich ACT products for

tumor-reactive T cells and, thereby, improve the efficacy of the current ACT strategies. Furthermore, the specific focus on this CD8⁺ T cell population can expedite the identification of therapeutically relevant TCRs. These strategies are highly promising to complement the current applicability of checkpoint blockade therapies.

Acknowledgements We thank M.G. Kallenberg-Lantrau and residents of the department of Pathology for the help with the collection of patient material.

Contributors JvdB cultured the bulk TIL, performed the *in vitro* assays, interpretation of all experiments and drafted the manuscript. MvdP provided experimental support. MEI ran the imaging mass cytometry assays and analysis. DR processed and analyzed the genomic data. RvdB collected patient material and prepared the genomic libraries. KCMJP was responsible for the patient recruitment and clinical supervision. AFS performed pathologic inspection of the tumors. TD was responsible for the isolation and expansion of CD8⁺ T cell subsets. EMEV and SHVdB have supervised T cell reactivity experiments. NFCCdM conceptualized this study, received funding, revised the manuscript and acts as guarantor.

Funding This work was supported by the European Research Council (ERC) under the European Union’s Horizon 2020 research and innovation program (grant agreement No. 852832). JvdB was supported by a LUMC PhD fellowship.

Competing interests TD and RD disclose that they submitted a patent regarding therapeutic and diagnostic use of the CD103⁺CD39⁺ CD8⁺ T cells in cancer patients. The other authors declare they have no competing interests.

Patient consent for publication Consent obtained directly from patient(s).

Ethics approval This study involves human participants and was approved by The Medical Ethical Committee of the Leiden University Medical Centre approved this study, protocol: P15.282. Participants gave informed consent to participate in the study before taking part.

Provenance and peer review Not commissioned; externally peer reviewed.

Data availability statement Data are available in a public, open access repository. All data relevant to the study are included in the article or uploaded as online supplemental information. Patient’s RNA sequencing data can be retrieved from the Sequence Read Archive of NCBI via PRJNA911749.

Supplemental material This content has been supplied by the author(s). It has not been vetted by BMJ Publishing Group Limited (BMJ) and may not have been peer-reviewed. Any opinions or recommendations discussed are solely those of the author(s) and are not endorsed by BMJ. BMJ disclaims all liability and responsibility arising from any reliance placed on the content. Where the content includes any translated material, BMJ does not warrant the accuracy and reliability of the translations (including but not limited to local regulations, clinical guidelines, terminology, drug names and drug dosages), and is not responsible for any error and/or omissions arising from translation and adaptation or otherwise.

Open access This is an open access article distributed in accordance with the Creative Commons Attribution Non Commercial (CC BY-NC 4.0) license, which permits others to distribute, remix, adapt, build upon this work non-commercially, and license their derivative works on different terms, provided the original work is properly cited, appropriate credit is given, any changes made indicated, and the use is non-commercial. See <http://creativecommons.org/licenses/by-nc/4.0/>.

ORCID iDs

Jitske van den Bulk <http://orcid.org/0000-0002-2056-9478>
 Els M E Verdegaal <http://orcid.org/0000-0002-4449-8707>
 Thomas Duhen <http://orcid.org/0000-0002-3043-9116>
 Noel F C C de Miranda <http://orcid.org/0000-0001-6122-1024>

REFERENCES

- Le DT, Durham JN, Smith KN, et al. Mismatch repair deficiency predicts response of solid tumors to PD-1 blockade. *Science* 2017;357:409–13.
- Overman MJ, McDermott R, Leach JL, et al. Nivolumab in patients with metastatic DNA mismatch repair-deficient or microsatellite instability-high colorectal cancer (checkmate 142): an open-label, multicentre, phase 2 study. *Lancet Oncol* 2017;18:1182–91.
- Chalabi M, Fanchi LF, Dijkstra KK, et al. Neoadjuvant immunotherapy leads to pathological responses in MMR-proficient and MMR-deficient early-stage colon cancers. *Nat Med* 2020;26:566–76.

- 4 Cerck A, Lumish M, Sinopoli J, et al. Pd-1 blockade in mismatch repair-deficient, locally advanced rectal cancer. *N Engl J Med* 2022;386:2363–76.
- 5 Samstein RM, Lee C-H, Shoushtari AN, et al. Tumor mutational load predicts survival after immunotherapy across multiple cancer types. *Nat Genet* 2019;51:202–6.
- 6 van den Bulk J, Verdegaal EME, Ruano D, et al. Neoantigen-specific immunity in low mutation burden colorectal cancers of the consensus molecular subtype 4. *Genome Med* 2019;11:87.
- 7 Parkhurst MR, Robbins PF, Tran E, et al. Unique neoantigens arise from somatic mutations in patients with gastrointestinal cancers. *Cancer Discov* 2019;9:1022–35.
- 8 Gros A, Tran E, Parkhurst MR, et al. Recognition of human gastrointestinal cancer neoantigens by circulating PD-1+ lymphocytes. *J Clin Invest* 2019;129:4992–5004.
- 9 Rajamanickam V, Ballesteros-Merino C, Samson K, et al. Robust antitumor immunity in a patient with metastatic colorectal cancer treated with cytotoxic regimens. *Cancer Immunol Res* 2021;9:602–11.
- 10 Yarchoan M, Hopkins A, Jaffee EM. Tumor mutational burden and response rate to PD-1 inhibition. *N Engl J Med* 2017;377:2500–1.
- 11 Tran E, Turcotte S, Gros A, et al. Cancer immunotherapy based on mutation-specific CD4+ T cells in a patient with epithelial cancer. *Science* 2014;344:641–5.
- 12 Bobisse S, Genolet R, Roberti A, et al. Sensitive and frequent identification of high avidity neo-epitope specific CD8 + T cells in immunotherapy-naïve ovarian cancer. *Nat Commun* 2018;9:1092.
- 13 Keskin DB, Anandappa AJ, Sun J, et al. Neoantigen vaccine generates intratumoral T cell responses in phase Ia glioblastoma trial. *Nature* 2019;565:234–9.
- 14 Zacharakis N, Huq LM, Seitter SJ, et al. Breast cancers are immunogenic: immunologic analyses and a phase II pilot clinical trial using mutation-reactive autologous lymphocytes. *J Clin Oncol* 2022;40:1741–54.
- 15 Rosenberg SA, Packard BS, Aebersold PM, et al. Use of tumor-infiltrating lymphocytes and interleukin-2 in the immunotherapy of patients with metastatic melanoma. A preliminary report. *N Engl J Med* 1988;319:1676–80.
- 16 Dudley ME, Wunderlich JR, Shelton TE, et al. Generation of tumor-infiltrating lymphocyte cultures for use in adoptive transfer therapy for melanoma patients. *J Immunother* 2003;26:332–42.
- 17 Verdegaal EME, Visser M, Ramwadhdebé TH, et al. Successful treatment of metastatic melanoma by adoptive transfer of blood-derived polyclonal tumor-specific CD4+ and CD8+ T cells in combination with low-dose interferon-alpha. *Cancer Immunol Immunother* 2011;60:953–63.
- 18 Rosenberg SA, Yang JC, Sherry RM, et al. Durable complete responses in heavily pretreated patients with metastatic melanoma using T-cell transfer immunotherapy. *Clin Cancer Res* 2011;17:4550–7.
- 19 Dudley ME, Yang JC, Sherry R, et al. Adoptive cell therapy for patients with metastatic melanoma: evaluation of intensive myeloablative chemoradiation preparative regimens. *J Clin Oncol* 2008;26:5233–9.
- 20 Stevanović S, Draper LM, Langhan MM, et al. Complete regression of metastatic cervical cancer after treatment with human papillomavirus-targeted tumor-infiltrating T cells. *J Clin Oncol* 2015;33:1543–50.
- 21 Tran E, Ahmadzadeh M, Lu Y-C, et al. Immunogenicity of somatic mutations in human gastrointestinal cancers. *Science* 2015;350:1387–90.
- 22 Poschke IC, Hassel JC, Rodriguez-Ehrenfried A, et al. The outcome of ex vivo TIL expansion is highly influenced by spatial heterogeneity of the tumor T-cell repertoire and differences in intrinsic in vitro growth capacity between T-cell clones. *Clin Cancer Res* 2020;26:4289–301.
- 23 Tran E, Robbins PF, Lu Y-C, et al. T-Cell transfer therapy targeting mutant KRAS in cancer. *N Engl J Med* 2016;375:2255–62.
- 24 Webb JR, Milne K, Watson P, et al. Tumor-Infiltrating lymphocytes expressing the tissue resident memory marker CD103 are associated with increased survival in high-grade serous ovarian cancer. *Clin Cancer Res* 2014;20:434–44.
- 25 Ye Q, Song D-G, Poussin M, et al. Cd137 accurately identifies and enriches for naturally occurring tumor-reactive T cells in tumor. *Clin Cancer Res* 2014;20:44–55.
- 26 Gros A, Robbins PF, Yao X, et al. Pd-1 identifies the patient-specific CD8PD-1 identifies the patient-specific CD8. *J Clin Invest* 2014;124:2246–59.
- 27 Simoni Y, Becht E, Fehlings M, et al. Bystander CD8+ T cells are abundant and phenotypically distinct in human tumour infiltrates. *Nature* 2018;557:575–9.
- 28 Thommen DS, Koelzer VH, Herzig P, et al. A transcriptionally and functionally distinct PD-1+ CD8+ T cell pool with predictive potential in non-small-cell lung cancer treated with PD-1 blockade. *Nat Med* 2018;24:994–1004.
- 29 Yossef R, Tran E, Deniger DC, et al. Enhanced detection of neoantigen-reactive T cells targeting unique and shared oncogenes for personalized cancer immunotherapy. *JCI Insight* 2018;3:e122467:19.:.
- 30 Kortekaas KE, Santegoets SJ, Sturm G, et al. CD39 identifies the CD4+ tumor-specific T-cell population in human cancer. *Cancer Immunology Research* 2020;8:10.
- 31 Krishna S, Lowry FJ, Copeland AR, et al. Stem-Like CD8 T cells mediate response of adoptive cell immunotherapy against human cancer. *Science* 2020;370:1328–34.
- 32 Balança C-C, Salvioni A, Scarlata C-M, et al. Pd-1 blockade restores helper activity of tumor-infiltrating, exhausted PD-1hiCD39+ CD4 T cells. *JCI Insight* 2021;6:e142513.
- 33 Eiva MA, Omran Chacon JA, et al. Systematic analysis of CD39, CD103, CD137, and PD-1 as biomarkers for naturally occurring tumor antigen-specific tils. *Eur J Immunol* 2022;52:96–108.
- 34 Duhen T, Duhen R, Montler R, et al. Co-Expression of CD39 and CD103 identifies tumor-reactive CD8 T cells in human solid tumors. *Nat Commun* 2018;9:2724.
- 35 Ceppek KL, Shaw SK, Parker CM, et al. Adhesion between epithelial cells and T lymphocytes mediated by E-cadherin and the alpha E beta 7 integrin. *Nature* 1994;372:190–3.
- 36 Gupta PK, Godec J, Wolski D, et al. Cd39 expression identifies terminally exhausted CD8+ T cells. *PLoS Pathog* 2015;11:e1005177.
- 37 Canale FP, Ramello MC, Núñez N, et al. Cd39 expression defines cell exhaustion in tumor-infiltrating CD8+ T cells. *Cancer Res* 2018;78:1115–28.
- 38 Ijsselsteijn ME, Petitprez F, Lacroix L, et al. Revisiting immune escape in colorectal cancer in the era of immunotherapy. *Br J Cancer* 2019;120:815–8.
- 39 Dobin A, Davis CA, Schlesinger F, et al. Star: ultrafast universal RNA-seq aligner. *Bioinformatics* 2013;29:15–21.
- 40 Li H. Aligning sequence reads, clone sequences and assembly contigs with BWA-MEM. *ArXiv* 2013.
- 41 Picard toolkit [Broad Institute, GitHub Repository]. 2019. Available: <http://broadinstitute.github.io/picard/>
- 42 McKenna N, Hanna M, Banks E, et al. The genome analysis toolkit: a MapReduce framework for analyzing next-generation DNA sequencing data. *Genome Res* 2010;20:1297–303.
- 43 Saunders CT, Wong WSW, Swamy S, et al. Strelka: accurate somatic small-variant calling from sequenced tumor-normal sample pairs. *Bioinformatics* 2012;28:1811–7.
- 44 Cibulskis K, Lawrence MS, Carter SL, et al. Sensitive detection of somatic point mutations in impure and heterogeneous cancer samples. *Nat Biotechnol* 2013;31:213–9.
- 45 Koboldt DC, Zhang Q, Larson DE, et al. VarScan 2: somatic mutation and copy number alteration discovery in cancer by exome sequencing. *Genome Res* 2012;22:568–76.
- 46 Lai Z, Markovets A, Ahdesmaki M, et al. VarDict: a novel and versatile variant caller for next-generation sequencing in cancer research. *Nucleic Acids Res* 2016;44:e108.
- 47 Khanna A, Larson DE, Srivatsan SN, et al. Bam-readcount -- rapid generation of basepair-resolution sequence metrics. *ArXiv* 2021;arXiv:2107.12817v1.
- 48 McLaren W, Gil L, Hunt SE, et al. The Ensembl variant effect predictor. *Genome Biol* 2016;17:122.
- 49 Robinson JT, Thorvaldsdóttir H, Winckler W, et al. Integrative genomics viewer. *Nat Biotechnol* 2011;29:24–6.
- 50 Thorvaldsdóttir H, Robinson JT, Mesirov JP. Integrative genomics viewer (IGV): high-performance genomics data visualization and exploration. *Briefings in Bioinformatics* 2013;14:178–92.
- 51 Robinson JT, Thorvaldsdóttir H, Wenger AM, et al. Variant review with the integrative genomics viewer. *Cancer Res* 2017;77:e31–4.
- 52 Ijsselsteijn ME, van der Breggen R, Farina Sarasqueta A, et al. A 40-marker panel for high dimensional characterization of cancer immune microenvironments by imaging mass cytometry. *Front Immunol* 2019;10:2534.
- 53 van den Bulk J, Verdegaal EM, de Miranda NF. Cancer immunotherapy: broadening the scope of targetable tumours. *Open Biol* 2018;8:180037.
- 54 Tauriello DVF, Palomo-Ponce S, Stork D, et al. Tgf β drives immune evasion in genetically reconstituted colon cancer metastasis. *Nature* 2018;554:538–43.
- 55 Wang Z-Q, Milne K, Derocher H, et al. CD103 and intratumoral immune response in breast cancer. *Clin Cancer Res* 2016;22:6290–7.
- 56 Komdeur FL, Wouters MCA, Workel HH, et al. CD103+ intraepithelial T cells in high-grade serous ovarian cancer are phenotypically



- diverse TCR $\alpha\beta+$ CD8 $\alpha\beta+$ T cells that can be targeted for cancer immunotherapy. *Oncotarget* 2016;7.
- 57 Banchereau R, Chitre AS, Scherl A, et al. Intratumoral CD103+ CD8+ T cells predict response to PD-L1 blockade. *J Immunother Cancer* 2021;9:e002231.
- 58 Shields BD, Koss B, Taylor EM, et al. Loss of E-cadherin inhibits CD103 antitumor activity and reduces checkpoint blockade responsiveness in melanoma. *Cancer Res* 2019;79:1113–23.
- 59 Scott AC, Dündar F, Zumbo P, et al. Tox is a critical regulator of tumour-specific T cell differentiation. *Nature* 2019;571:270–4.
- 60 Philip M, Schietinger A. Cd8+ T cell differentiation and dysfunction in cancer. *Nat Rev Immunol* 2022;22:209–23.
- 61 Leidner R, Sanjuan Silva N, Huang H, et al. Neoantigen T-cell receptor gene therapy in pancreatic cancer. *N Engl J Med* 2022;386:2112–9.
- 62 Li S, Zhuang S, Heit A, et al. Bystander CD4+ T cells infiltrate human tumors and are phenotypically distinct. *Oncolimmunology* 2022;11:2012961.
- 63 Lowery FJ, Krishna S, Yossef R, et al. Molecular signatures of antitumor neoantigen-reactive T cells from metastatic human cancers. *Science* 2022;375:877–84.
- 64 Duhen R, Fesneau O, Samson KA, et al. Pd-1 and ICOS coexpression identifies tumor-reactive CD4+ T cells in human solid tumors. *J Clin Invest* 2022;132:e156821.

Supporting documents

Figure S1 | Phenotypic analysis of the flow sorted CD8⁺ T cell subsets. A,B) Summary of T cell subset relative frequencies at flow sorting. The error bars represent the median with interquartile range. C-D) Frequency of CD8⁺ T cells that express CD69 (C), CD127 (D) or PD-1 (E) in each subset. The error bars represent the median with interquartile range. F) Mean fluorescence intensity of PD-1 expression on CD8 T cells. A-F) Each graph includes the result of an one-way ANOVA test.

Figure S2 | T cell reactivity screening. IFN- γ and granzyme B release was measured by ELISA in the supernatant of the co-culture assay for each patient, performed in two independent assays. Each T cell product is visualized by a distinct color: DP in yellow, SP39 red, SP(103) in blue, DN in black and bulk TIL in green. Potential epitopes are marked by an asterisk *. Positive (SEB) and negative (EBV-LCL with DMSO) controls are included at the far right of the graphs.

Figure S3 | Validation of potential neoantigen-specific T cell responses. The validation measurements are visualized for each patient, including IFN- γ , granzyme B and flow cytometric measures CD137 and OX40. T cell responses derived from the bulk TIL (green) or DP (yellow) are depicted against the corresponding wild-type peptide (grey) or a DMSO control (grey). The respective neo-epitope is listed within each graph.

Figure S4 | Intracellular IFN- γ expression in TIL after stimulation with neopeptides. A) Representative sample with increased IFN- γ expression specifically in the CD4⁺ T cells. B) Each graph depicts the percentage of IFN- γ ⁺ cells that were determined to be either CD4⁺ or CD8⁺ T cells per sample. NIC4 L29 was validated as a true CD8-mediated response, as it was also detected in the DP CD8⁺ T cell subset.

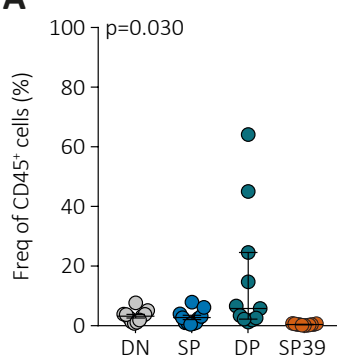
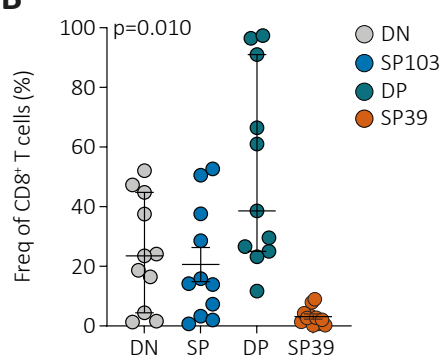
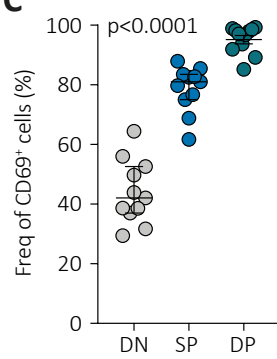
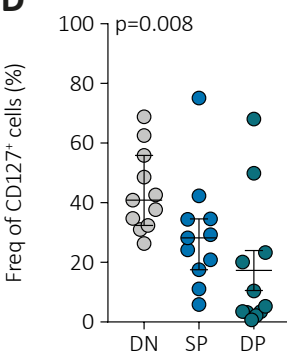
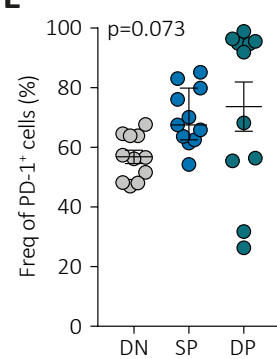
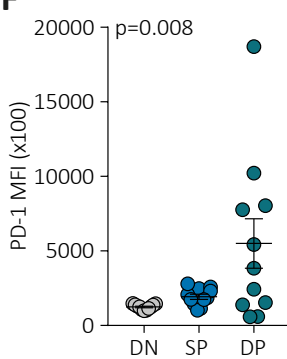
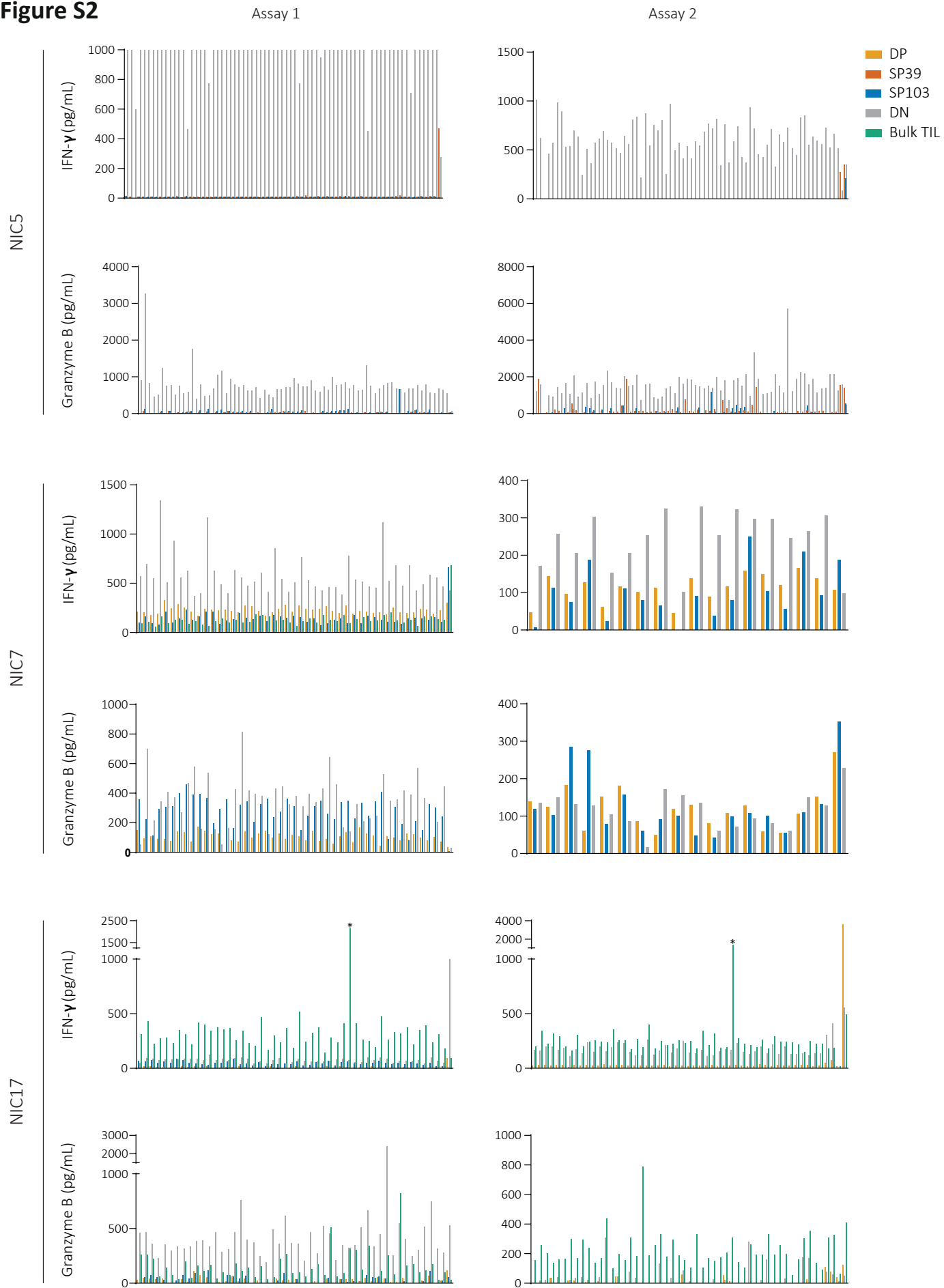
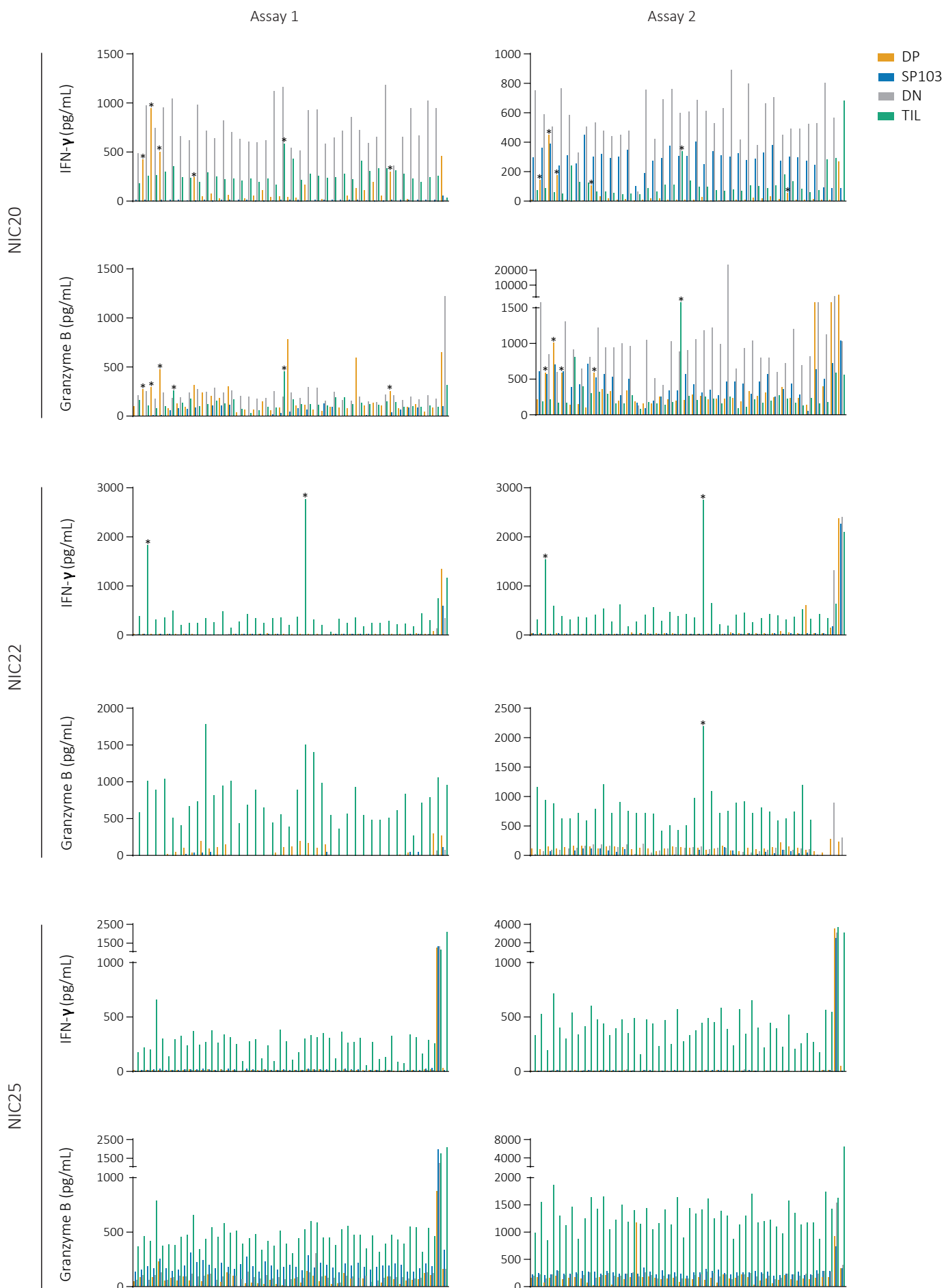
Figure S1**A****B****C****D****E****F**

Figure S2



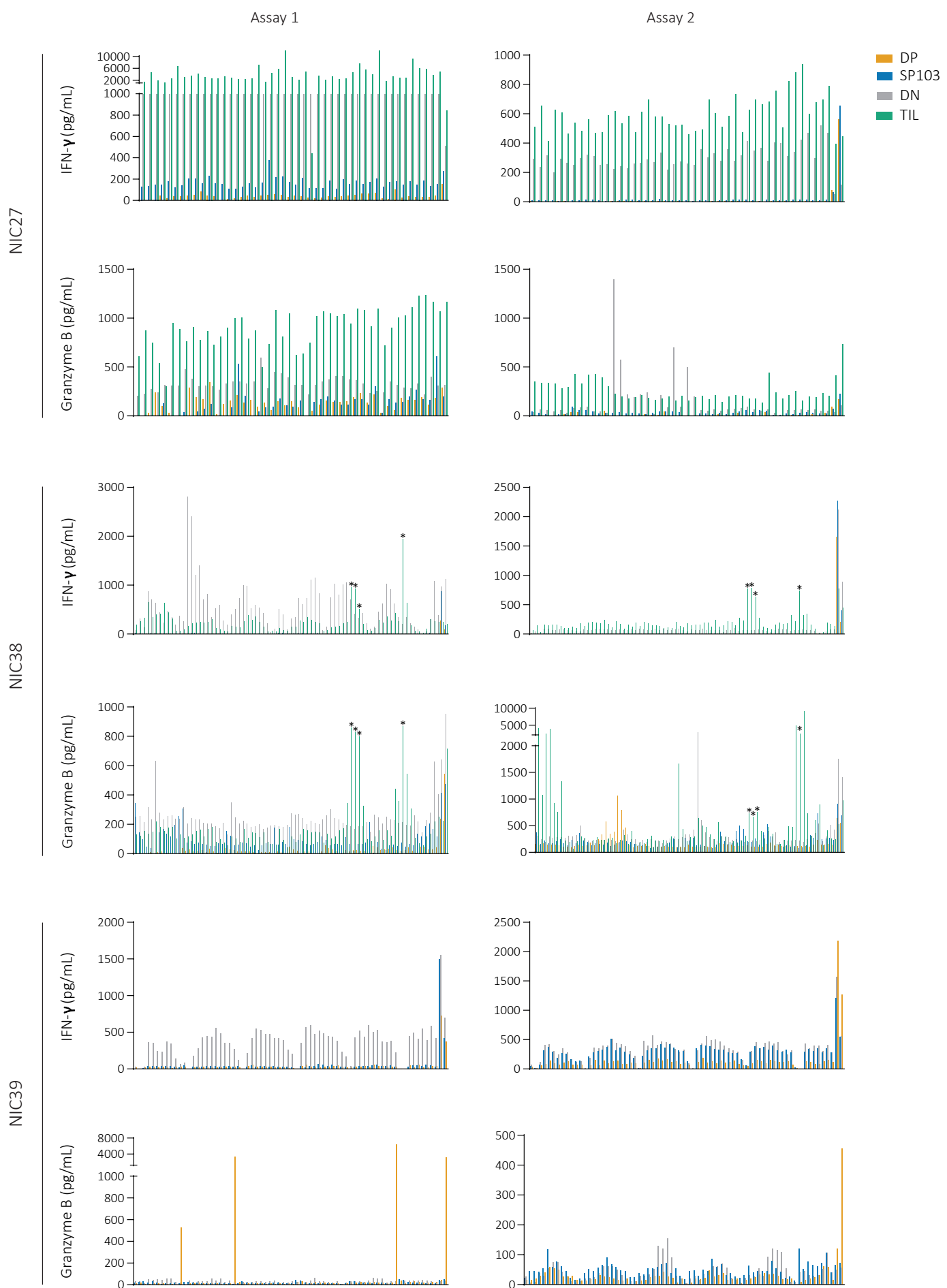


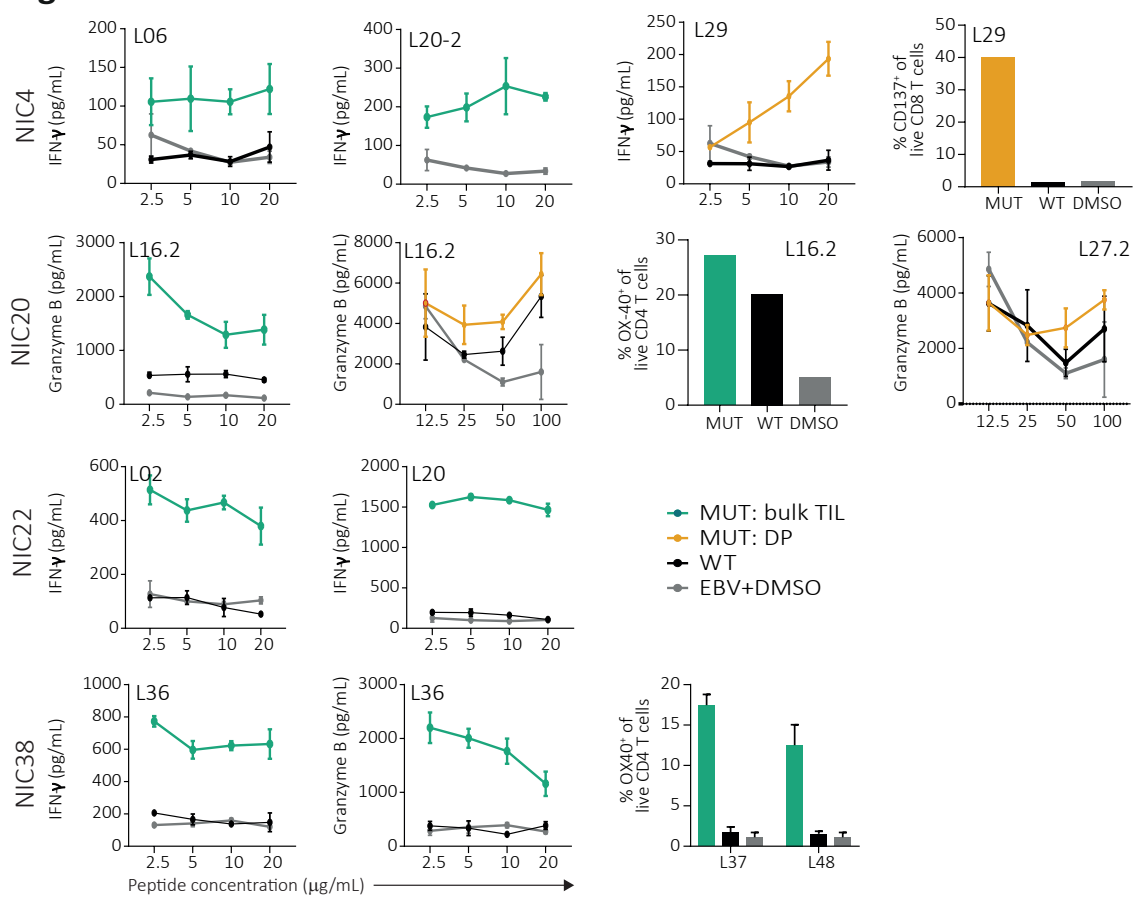
Figure S3

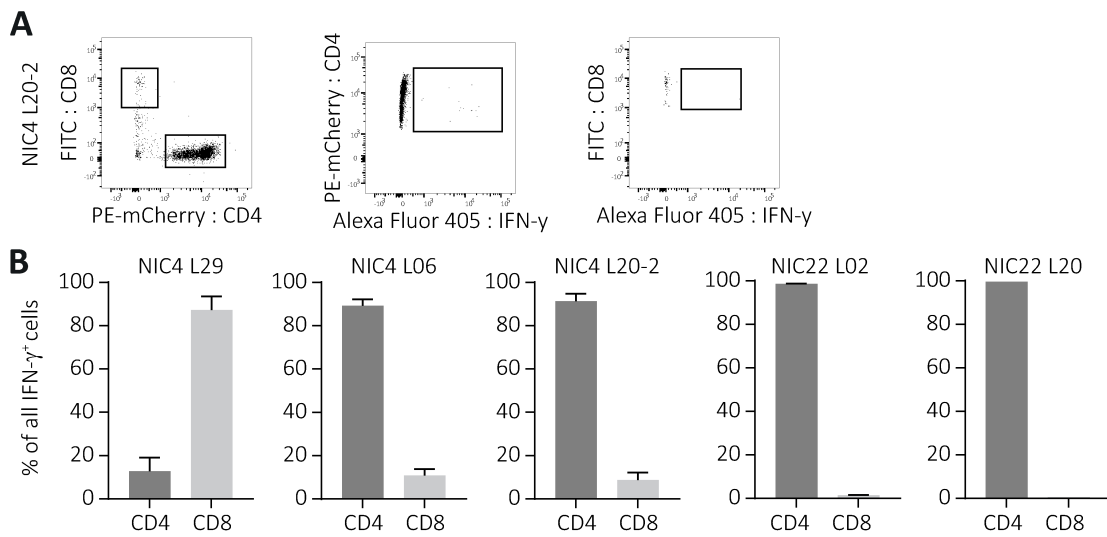
Figure S4

Table S1 | Percentage of CD4+ and CD8+ T cells in expanded bulk TIL cultures.

Patient ID	CD4 (%)	CD8 (%)
NIC4	81	19
NIC5	93	7
NIC7	92	8
NIC16	61	39
NIC17	34	66
NIC20	96	4
NIC22	50	50
NIC25	95	5
NIC27	60	40
NIC38	28	72
NIC39	99	1

Table S2 | All mutant peptide sequences that were investigated for T cell reactivity.

Patient ID	Mutational position	Mutation type	Gene	SLP ID	Peptide sequence
NIC4	chr1_11950386_G/A	Missense	<i>PLOD1</i>	L01	ADSYDVLFASGPQELLKKFRQARSQ
NIC4	chr11_14818305_G/A	Missense	<i>PDE3B</i>	L02	FPDTADFLNKPSIILQRSLGNAPNT
NIC4	chr11_74374521_C/T	Missense	<i>PGM2L1</i>	L03	ENLLRNGMNKEQDRLCCRMFTGTA
NIC4	chr11_86446352_G/A	Missense	<i>ME3</i>	L04	PGVALGVIAGGIWHPDEIFLLTAE
NIC4	chr12_25245347_C/T	Missense	<i>KRAS</i>	L05	YKLVVVGAGDVGKSAITIQLIQ
NIC4	chr14_58223625_G/A	Missense	<i>ACTR10</i>	L06	SVPEGVLEDIAHTCFVSDLKRGLK
NIC4	chr14_73276592_C/T	Missense	<i>NUMB</i>	L07	PSPTNPFFSSDLQKTFKIEL
NIC4	chr14_73276674_C/G	Missense	<i>NUMB</i>	L08	TGTCPVDPFEAQCAALENKSQRTN
NIC4	chr14_80792789_C/A	Missense	<i>CEP128</i>	L09	KLERALEKQSETFDELTGKNQNQLK
NIC4	chr16_28830704_G/C	Missense	<i>ATXN2L</i>	L10	GVRCSSSRGGRPALSSLPPRGPHHL
NIC4	chr17_42787309_A/G	Missense	<i>WNK4</i>	L11	EMVALGLVCEADCPVARAVRERVA
NIC4	chr17_44190551_G/A	Missense	<i>TMUB2</i>	L12	GQESQMKLIVQGHLLQDPARTLRLS
NIC4	chr17_63420571_G/A	Missense	<i>TANC2</i>	L13	PPPVGQQKEYPNPPPSPLRRGPQY
NIC4	chr17_7674221_G/A	Missense	<i>TP53</i>	L14	YMCNSSCMGGMNRWPIILTIILEDSSG
NIC4	chr19_10555328_CCTT/C	Inframe deletion	<i>KRI1</i>	L15	FGLSTEEILAADDDELNRWCSLKTCM
NIC4	chr19_1093973_G/A	Missense	<i>POLR2E</i>	L16	QFGDKPSEGPRRCTDLTVLVAHNDD
NIC4	chr19_13074002_C/A	Missense	<i>NFIX</i>	L17	YYNINQVTLGRRYITSPPSTTTR
NIC4	chr2_219615172_C/T	Missense	<i>STK11P</i>	L18	TLFLLEDAAGSLAEPSPPAASGEA
NIC4	chr2_74889415_G/A	Missense	<i>HK2</i>	L19	AGMAAVVDRIRENHGLDAALKVTVG
NIC4	chr20_57378098_A/G	Stop loss	<i>RAE1</i>	L20-1	NAAEELPKRNKKWWLETLAQPELFL
				L20-2	WWLETLAQPELFSTLPHLCNLGP
				L20-3	LSTLPHLCNLGPSLVGLSAMDMDF
				L20-4	PSLVGLSAMDMDFNPWRKRCHCSAA
				L20-5	FNPWRKRCHCSAAESPVGVRGDLPSL
				L20-6	SAAESPVGVRGDLPSLHSTACCRVFL
NIC4	chr3_11259275_G/A	Missense	<i>HRH1</i>	L21	SLSVADLIVGAVIMPMMNLYLLMSK
NIC4	chr3_192144025_T/G	Missense	<i>FGF12</i>	L22	SGPTMNGGKVVTQDST
NIC4	chr3_37298887_G/A	Missense	<i>GOLGA4</i>	L23	VKTLETLQQRVKHQEENLLRKCKETI
NIC4	chr4_143185536_C/T	Missense	<i>USP38</i>	L24	LKRVIVRKVVESVEHWLDEAQCEAM
NIC4	chr5_103028911_T/A	Missense	<i>PAM</i>	L25	GRFRKGSGGLNHGNFFASRKGYSR
NIC4	chr5_112838150_GGA/G	Frameshift	<i>APC</i>	L26-1	SSRSEKDRSLERTRNWSRQLPSSNR
				L26-2	TRNWSRQLPSSNRKSRNFFKARFAD
				L26-3	RKSRNFFKARFADLHHCSPDCQSHG
				L26-4	DLHHCSPDCQSHGRSVSHYLSGRQ
				L26-5	PDCQSHGRSVSHYLSGRQKFVWYH
NIC4	chr7_94400200_C/T	Missense	<i>COL1A2</i>	L27	PAGDRGPRGERGLPGPPGRDGEDGP
NIC4	chr8_142613268_C/T	Missense	<i>ARC</i>	L28	QYVVGTLQPKLKHFLRHLPLPKTEQ
NIC4	chr8_93923083_C/T	Missense	<i>PDP1</i>	L29	PKSEAKSVVKQDWLLGLMPFRAFG
NIC4	chrX_1593799_C/T	Missense	<i>AKAP17A</i>	L30	IKLSGFSDILKVCAAEIFKIDFPTRH
NIC5	chr1_171584051_A/C	Missense	<i>PRRC2C</i>	L01	TAIHNFPTVHQALAKAQSGLAFQQ
NIC5	chr1_207767803_C/T	Missense	<i>CD46</i>	L02-1	LSHSVSTSSTTKFPASSASGPRPTY
				L02-2	KCLKVSTSSTTKFPASSASGPRPTY
				L02-3	KCLKVSTSSTTKFPASSASGYPKPE
NIC5	chr1_209783196_G/C	Missense	<i>C1orf74</i>	L03	LKALVAEIIITHLEGLQRDSLAVSY
NIC5	chr1_46270754_C/T	Missense	<i>RAD54L</i>	L04	AASEADRQLGEEWLRELTISVNRL
NIC5	chr1_90027699_T/G	Stop lost	<i>ZNF326</i>	L05-1	EELLEETAKEPADFPVEQPEENEI
				L05-2	PADFPVEQPEENEI
NIC5	chr10_114575476_T/A	Missense	<i>ABLIM1</i>	L06	TRCHGCGEFVEGVVVVTALGKTYHPN
NIC5	chr10_73915266_C/T	Missense	<i>PLAU</i>	L07	GFGKENSTDYLYLEQLKMTVVKLIS
NIC5	chr11_66020856_T/A	Missense	<i>CATSPER1</i>	L08	IFTTIFTLFTLSSLDWDWSLIYMDSR
NIC5	chr11_67999580_C/T	Missense	<i>UNC93B1</i>	L09	NYWERYYTLPSTVALGMAIVPLWA
NIC5	chr11_95783089_T/A	Missense	<i>FAM76B</i>	L10-1	HPKHHHHHHHHHLRHSSSHHK1NSL
				L10-2	RKTSIIQNIITIIITFVTAVAT
NIC5	chr13_45525021_A/G	Missense	<i>COG3</i>	L11-1	LKTMASQGGPKYALSQWPWAQPAVK
				L11-2	VKNNGQSGRPQVCSLAALGTTSKG
NIC5	chr13_98809435_G/A	Missense	<i>DOCK9</i>	L12	FERLAHYDTLHWAYSKVTEVMHSG
NIC5	chr14_103135969_G/A	Missense	<i>TNFAIP2</i>	L13	VSTASIRRHIQVAPQPLQAGPAMGP
NIC5	chr14_64065516_G/A	Missense	<i>SYNE2</i>	L14	RQILRLLRLRCTKNDGICLLKIVSA
NIC5	chr15_41669457_A/T	Missense	<i>MGA</i>	L15	FYKLKLTNNNTLDLEGIIHLHSMHYR
NIC5	chr16_346835_G/A	Missense	<i>AXIN1</i>	L16	IKGETSTATPTRLDDLGYEPEGSA
NIC5	chr16_88631239_G/T	Missense	<i>ZC3H18</i>	L17	ASTLSRREEELLKHLKAVEDAICKR
NIC5	chr17_31233211_TG/T	Frameshift	<i>NF1</i>	L18	MMGDQGEELPIAMALANVPCSQWMN
NIC5	chr17_39725079_G/A	Missense	<i>ERBB2</i>	L19	AKGMSYLEDVRLIHRDLAARNVLVK
NIC5	chr17_48860426_T/C	Missense	<i>CALCCO2</i>	L20	TSDEGGARONPGPAYGNPYSGIQES
NIC5	chr17_58357951_G/A	Missense	<i>RNF43</i>	L21	QVTRSNSAAPSGWLSNPQCPRALPE
NIC5	chr17_7673776_G/A	Missense	<i>TP53</i>	L22	FEVRVCACPGRDWRTEEENLRKKGE
NIC5	chr19_48441818_C/T	Missense	<i>GRIN2D</i>	L23	FIYDAAVLNMYMACKDEGCKLVTIGS
NIC5	chr19_49447035_G/C	Missense	<i>PIH1D1</i>	L24-1	LEAPDLLLAEVDVPKLDGALGLSLE
				L24-2	LEAPDLLLAEVDVPKLDGALGLSLE

NIC5	chr19_55401666_G/A	Missense	<i>UBE2S</i>	L24-3	HLNLWLEAPDLLAEIDVPKLTQI
NIC5	chr2_110144543_C/G	Missense	<i>NPHP1</i>	L24-4	LEAPDLLAEIDVPKLINSHESKAA
NIC5	chr2_127050828_C/A	Missense	<i>BIN1</i>	L25	RLLLENYEEYAAWARLLEIHHGAG
NIC5	chr2_127426153_G/A	Missense	<i>PROC</i>	L26	IPAKTYELFLNGATPYEKGIEVDP
NIC5	chr2_240462422_A/T	Missense	<i>GPC1</i>	L27	GTVEGGSGAGRQLYLPPGFMFKVQAQ
NIC5	chr2_96298337_G/C	Missense	<i>SNRNP200</i>	L28	MEKKRSHLKRDTKDQEDQVDPRLID
NIC5	chr20_18183172_C/T	Missense	<i>KAT14</i>	L29	LFKQLHPOLLLVDYLDCLGKQAEA
NIC5	chr20_46374418_C/T	Missense	<i>ELMO2</i>	L30	ERIMGKMEADPEVKFLQLYHETEK
NIC5	chr3_197065340_G/A	Missense	<i>DLG1</i>	L31	TKPPKLQLLSQICSHLHRSDPHWTP
NIC5	chr4_139370290_G/C	Missense	<i>NAA15</i>	L32	DTYIRIVLENSSQEDKHECPGRSA
NIC5	chr4_148120260_C/T	Missense	<i>NR3C2</i>	L33	MEKDIQEHKFIEVGQYNNHHLYGTSV
NIC5	chr5_112839398_AAT/A	Frameshift	<i>APC</i>	L34	QRRAQKKAQIEEDKNAEKEKQQRN
NIC5	chr5_112839906_AC/A	Frameshift	<i>APC</i>	L35-1	NLGERRCISLPCINYARGCTKSAFS
				L35-2	FNEEKMHQSAMYKLCQGMHQISLQF
NIC5	chr5_138924582_G/A	Missense	<i>CTNNA1</i>	L36	CKVSSINQETIOTYCVEDTPMFFKM
NIC5	chr5_157809736_G/A	Missense	<i>CLINT1</i>	L37-1	SPGQTMPPSRSKNLHHLLKQLKPSE
NIC5	chr6_105282511_C/G	Missense	<i>PREP</i>	L37-2	KNLHHLLKQLKPSEKYLKIKHLLK
NIC5	chr6_135463154_G/T	Missense	<i>AHI1</i>	L37-3	KPSEKYLKIKHLLKRERVDSLKLQ
NIC5	chr6_136356706_T/A	Missense	<i>MAP7</i>	L38	IALQEKKDVGQLDHTAGAIRGRAARV
NIC5	chr6_168078950_T/A	Missense	<i>FRMD1</i>	L39	WDEEWDKNKSASFDSKLGELSDKI
NIC5	chr6_26413488_G/T	Missense	<i>BTN3A1</i>	L40	DFQCAAEEYLIKERYTSPKRLTINGG
NIC5	chr7_76625578_T_TTTCTCC	Inframe insertion	<i>POMZP3</i>	L41	TEDSMQDDTKPKQKTKKKTKAVAD
NIC5	chr7_99454126_C/G	Missense	<i>CPSF4</i>	L42	VGSPHVVTSHQSNTVTESTPDLKEQ
				L43	CSQQEPTLGM DALASEHRDVLLP
NIC5	chr8_100153299_G/A	Missense	<i>POLR2K</i>	L44	GLTDGNKYRTLTDPRTNLKLKPPK
NIC5	chr8_37899408_C/A	Missense	<i>RAB11FIP1</i>	L45	TVLSALKEKKKEKRTVEEEDQIFL
NIC5	chr8_73673126_G/C	Missense	<i>STAU2</i>	L46-1	AGNRGPRPLEQVSCYKCGEKGHYAN
				L46-2	AGNRGPRPLEQVSCYKCCCLSLFP
				L46-3	RATGDPGHWSRSAVTSVARKDTTPT
NIC5	chr9_114169425_A/G	Missense	<i>COL27A1</i>	L47	IRCRECGYRIMYKRTKRLVIFDAR
NIC5	chr9_134050430_G/T	Missense	<i>BRD3</i>	L48	MSLMVSAGRGLWAVWSPTHQVTVL
NIC5	chr9_134690995_C/T	Missense	<i>COL5A1</i>	L49-1	KPFPNYRANYNFGGMYMNQRYHCPVP
NIC5	chr9_136946680_G/A	Missense	<i>C8G</i>	L49-2	KPFPNYRANYNFGGMYMNQRWQHNG
NIC5	chr9_19378868_C/T	Missense	<i>RPS6</i>	L49-3	YRPLDPKPFPNYRANYNFGGMYNR
NIC5	chrX_49065811_G/A	Missense	<i>CCDC120</i>	L50	FHLAGSTPFLVGPPGPKGDCGLP
NIC5	chr4_141222377_TA/T	Frameshift	<i>ZNF330</i>	L51	VTSPVPVPPAAAPTTPATPVPVPP
NIC7	chr1_166858202_C/A	Missense	<i>TADA1</i>	L52	DGITKTTGFCATWRSSKGPDVAYRV
NIC7	chr1_173984497_A/T	Splice	<i>RC3H1</i>	L53	QIFYFPKYGCFCEAADQFHILDEVRR
				L54	RISGGNDKQGFPIKQGVLTGHRVRL
NIC7	chr1_206195806_A/C	Missense	<i>FAM72A</i>	L55	SSFEGRSVPATPLRGAGPQLCKP
NIC7	chr1_224294313_C/T	Missense	<i>NVL</i>	L56	MPKKRLVRGRRRLTAENVKNN
NIC7	chr1_32091892_C/T	Missense	<i>TMEM39B</i>	L01	SHPPPDDAEQQASLLLACSGDTLP
				L02-1	LALYLKPLSSARGKFVFSYLSKST
NIC7	chr1_51302546_G/A	Missense	<i>TTC39A</i>	L02-2	RGKVFVSYLSKTAFFKYSVHNPI
NIC7	chr1_7778152_T_TCAG	Inframe insertion	<i>VAMP3</i>	L03	CSSCLLSCNCINGHVWMFHSQLYDIN
NIC7	chr10_112425377_T/G	Missense	<i>ACSL5</i>	L04	SLDPALRRAGRFNREICLGPDEAS
NIC7	chr10_472477_C/A	Missense	<i>DIP2C</i>	L05-1	AMPTHACCLSPSFIRSEVEFLKMDF
NIC7	chr10_47922844_G/T	Missense	<i>CH17-3605.1</i>	L05-2	LOHAKTAVWPGRHAHPCLPVTQLHPQ
NIC7	chr10_50814032_G/A	Missense	<i>A1CF</i>	L06	FVLGTGNVNIEEVEKLLKPYLNRYP
				L07	KMWAIGITVLVIFSIIIIVVVSS
NIC7	chr11_59152054_G/A	Missense	<i>FAM111A</i>	L08	GTLKIIIDRKKNIVKLAQGEYIAPEK
NIC7	chr12_16363960_T/G	Missense	<i>MGST1</i>	L09	PVTPTSSASRYHRLRSSGSRDERYRS
NIC7	chr12_1754359_GAA/G	Frameshift	<i>ADIPOR2</i>	L10	FAVLWLPLHVFNILEDWHEAIPIC
				L11-1	RAIIRAPSVRGAVGVVRGLGGRGYLA
NIC7	chr12_56257327_G/A	Missense	<i>ANKRD52</i>	L11-2	VREIYMNVPVGAVGVVRGLGGRGYLA
NIC7	chr13_109783442_C/T	Missense	<i>IRS2</i>	L12	EIETHQQGEMLVHGTEGIKEYINLG
NIC7	chr13_113766192_G/A	Missense	<i>TMEM255B</i>	L13	HTIAYLTPLPQPKRALSFVGVYGV
NIC7	chr16_72950933_C/T	Missense	<i>ZFHX3</i>	L14-1	MNEPTAPIGVQQQDSRARYKAQKRAP
				L14-2	IGVQQDSRARYKAQKRAPTGWT
NIC7	chr17_7676002_TCA/T	Frameshift	<i>TP53</i>	L15	LDQERRTPLHAAYVGDVPLQLLL
				L16	TQPPHPVVPSPVQPSGGRPREGFLGQ
NIC7	chr19_39879805_G/A	Missense	<i>FCGBP</i>	L17	GSLLLVSVLIVITGLAATTRTENV
				L18-1	LVGGEIPLDMRLRGQQLVSEELMNL
				L18-2	MRLRGQQLVSEELMNLGESFIQTN
NIC7				L19-1	RLGFLHSGTAKSDLHVLPCPQQDVL
				L19-2	SDLHVLPCPQQDVLPTGQDLP
				L19-3	CAAV
				L19-4	YQGSYGFRLGFLHSGTAKSDLHVL
				L19-5	P
				L19-6	RLGFLHSGTAKSDLHVLPTGQDLP
				L20	HSGTAKSDLHVLPTGQDLP
					CAAV
					GGQGVCLPNYEAMCWLWGDPHYHSF

NIC7	chr19_55093057_C/T	Missense	<i>PPP1R12C</i>	L21	KPAQSLDPSRRPHVPGVENSDSAQ
NIC7	chr2_240464953_C/A	Missense	<i>GPC1</i>	L22	RRRGKLAPRERPHSGTLEKLVSEAK
NIC7	chr20_34776325_C/T	Missense	<i>NCOA6</i>	L23	LRILAQSNNNQLQDGLGILSVQIEGE
NIC7	chr20_35044541_A/C	Missense	<i>TRPC4AP</i>	L24	TLLAKNAQQKKSVLGSPAAEINQA
NIC7	chr22_17108607_C/T	Missense	<i>IL17RA</i>	L25	TRAKWQALLGRGVPVRLRCDHGKPV
NIC7	chr3_101857345_G/T	Missense	<i>NFKBIZ</i>	L26	TALHVAASLQYRFTQLDAVRLLMRK
NIC7	chr4_13602515_C/T	Missense	<i>BOD1L1</i>	L27	KYAETVKLKHKRNPKGKVKDIDIVE
NIC7	chr7_129413686_G/A	Missense	<i>AHCYL2</i>	L28	VCNMGHNSTEIDMASLRTPELTWER
NIC7	chr8_66429486_C/A	Missense	<i>RRS1</i>	L29	RPRPLTRWQQFAILKGIRPKKKTNL
NIC7	chrM_15617_G/A	Missense	<i>MT-CYB</i>	L30	TILRSVPNKLLGILALLSILILAM
NIC7	chrX_54541327_C/T	Missense	<i>GNL3L</i>	L31	KQQAAREQERQKCRRTIESYCQDVR
NIC7	chr19_48195980_G/A	Missense	<i>C19orf68</i>	L32	WRGAQLHDERAGELRTAEWKGPOSE
NIC7	chr1_18910469_C/T	Missense	<i>IFFO2</i>	L33-1	CNPTIDLQGEKLATAKSMDMNRLH
				L33-2	KEYQETIGQIELKLATAKSMDMNRLH
NIC16	chr10_102366504_A/T	Missense	<i>GBF1</i>	L01	IQRLLAEFTERWLNCNGSPFANSDA
NIC16	chr1_114713909_G/T	Missense	<i>NRAS</i>	L02	ETCLLDILDTAGKEEYSAMRDQYMR
NIC16	chr11_2270166_TTCGCCCGCCTACGGCCGC/T	Frameshift	<i>ASCL2</i>	L03	RRPATAETGGGAMSASATA
NIC16	chr1_156956504_C/G	Missense	<i>ARHGEF11</i>	L04	NTYMSHAGIRLDRAPSNTAEKAQS
NIC16	chr11_65635326_C/A	Missense	<i>PCNX3</i>	L05	RLVISHEGDPAWSSAILNSTPSSL
NIC16	chr12_123627113_A/G	Missense	<i>EIF2B1</i>	L06	LTHAYSRVVLRVPEAAVAAKKRFSV
NIC16	chr12_57769824_C/T	Missense	<i>METTL1</i>	L07	RAAPAGGFQNIAYLRSNAMKHLNF
NIC16	chr12_65169982_C/A	Missense	<i>LEMD3</i>	L08	SLGGPGGASAAGHSKVLLFSS
NIC16	chr16_15724685_G/T	Missense	<i>MYH11</i>	L09	LQDQLDEEMEAKKNLERHISTLNIQ
NIC16	chr17_29583013_C/A	Missense	<i>GIT1</i>	L10.1	TLLQMVTLASNWANSIWEHSLLDP
				L10.2	MVHTLASNWANSIWEHSLLDPAQVQ
NIC16	chr17_75836605_G/A	Missense	<i>UNC13D</i>	L11	IRRFRSVFPLSVLDSPARLQLSLRV
NIC16	chr17_79077832_T/G	Missense	<i>ENGASE</i>	L12.1	PPLSSQRPRTLWHDMMMGYLLDRD
				L12.2	PPLSSQRPRTLWHDMMMGYLLDRD
NIC16	chr19_57873985_A/T	Missense	<i>ZNF814</i>	L13	VHAGERPFKCGESVKSFSHKRSLVH
NIC16	chr2_106843518_C/T	Missense	<i>ST6GAL2</i>	L14	SHTQGTLGPSPREPGPREGAFPAA
NIC16	chr2_130172479_C/A	Missense	<i>SMPD4</i>	L15	LITQKPLPVSLHFRTSDCAYFLVD
NIC16	chr2_238140762_G/A	Missense	<i>KLHL30</i>	L16	MVQNVDLDFHLPASHAQDMGLQR
NIC16	chr22_38699959_TTG/T	Frameshift	<i>JOSD1</i>	L17	MSCVPWKGEQI
NIC16	chr2_70088042_T/A	Missense	<i>PCBP1</i>	L18	TNSTAASRPPVTQRLVVATQCGSL
NIC16	chr5_112827969_TG/T	Missense	<i>APC</i>	L19	LCSMKGCMRALVPN
NIC16	chr5_37726991_G/A	Missense	<i>WDR70</i>	L20	KTDDSNPREAILHHAKAAEDSPYVV
NIC16	chr6_33687091_G/A	Missense	<i>ITPR3</i>	L21	DSENAERILISLQPQELVDVIKKAY
NIC17	chr10_133370734_C/T	Missense	<i>ECHS1</i>	L01	PFASGANFEIITEKRGKNNNTVGLI
NIC17	chr10_72935651_C/A	Missense	<i>PLA2G12B</i>	L02	TLGCRPFMNSQRAAFCAEEKEEL
NIC17	chr1_116589057_C/T	Missense	<i>IGSF3</i>	L03	QVSKSKRLLTVKNKPIQLNCVKS
NIC17	chr11_17169117_G/C	Missense	<i>PIK3C2A</i>	L04	SYPLTPATPFHPEGSLPIYRPVVST
NIC17	chr11_2570678_G/C	Missense	<i>KCNQ1</i>	L05	VVFFGTEYVVRILCSAGCRSKYVGWL
NIC17	chr11_6683217_T/C	Missense	<i>MRPL17</i>	L06	FRRMGLGPESIRLRLNLLTGLVRH
NIC17	chr1_26122123_T/C	Missense	<i>PDIK1L</i>	L07.1	TSDLEPTLKVADSGLSKVCASGQN
				L07.2	PDNLISQTRLDTSLEPTLKVADS
NIC17	chr12_6750194_G/A	Missense	<i>MLF2</i>	L08.1	GAPKVYQETSEMCSAPGGIRETRRT
				L08.2	GAPKVYQETSEMCSAPGGVSWGALL
NIC17	chr13_102821834_A/G	Missense	<i>BIVM</i>	L09	FEDIRFGPFTGNATLMRWFHQINDH
NIC17	chr13_30657546_C/T	Missense	<i>USPL1</i>	L10	CSERHKKFEPALEIHIVIWERKIS
NIC17	chr14_21230984_T/A	Missense	<i>HNRNPC</i>	L11.1	KRSAAEMYGSVTDHPSPSPLSSSF
				L11.2	KRSAAEMYGSVTDHPSPSPLSVYQ
NIC17	chr1_44802975_G/A	Missense	<i>PLK3</i>	L12	SLGCVMYTLLCGNPPFETADLKETY
NIC17	chr15_44651635_G/C	Missense	<i>SPG11</i>	L13	ELKCVSVTGTAVFTWEVERMGYTI
NIC17	chr15_68086601_C/T	Missense	<i>PIAS1</i>	L14	PQLTYDGHPASSLLLVLPSVLLGPKE
NIC17	chr16_19699568_C/T	Missense	<i>C19orf62</i>	L15	SFFNSILAHGDLCNNLNQLSVNLW
NIC17	chr16_2175867_G/T	Missense	<i>TRAFF7</i>	L16	KIWDITLDCIHFQLQTSGGSVYSIS
NIC17	chr1_6469615_G/A	Missense	<i>PLEKHG5</i>	L17	TDLLLVTKAVKKVERTRVIRPPLL
NIC17	chr16_67167533_C/T	Missense	<i>HSF4</i>	L18	GLSPHRARGPIFDIPEDSPSPEGT
NIC17	chr1_68137792_C/A	Missense	<i>WLS</i>	L19.1	FLYAPSHKNYGEYQSNGDVGHSQE
				L19.2	FLYAPSHKNYGEYQSNGMQLPCKSR
NIC17	chr17_82054677_G/A	Missense	<i>GPS1</i>	L20	NYKGNSIKESIRGHDDLGDHYLDC
NIC17	chr18_58919969_C/T	Missense	<i>ZNF532</i>	L21	QQIKOAIINAAALQOPPKVSRVQVV
NIC17	chr19_11021837_C/T	Missense	<i>SMARCA4</i>	L22	NTHYVAPRRLLMGTPQLNKLPELW
NIC17	chr19_3478879_C/T	Missense	<i>SMIM24</i>	L23	LKPWLVGLAAVSVFLIVYLVLLAN
NIC17	chr19_47680387_G/T	Missense	<i>GLTSCR1</i>	L24	PQNLTTFMAAGKAVQNVVLSGFPAPA
NIC17	chr19_55092787_G/A	Missense	<i>PPP1R12C</i>	L25	EHRKVGKEWRGPVEGEAEPADRSQ
NIC17	chr19_55482650_A/C	Missense	<i>ZNF628</i>	L26	RDHTGERPYQCGACGKAFKRSSLLA
NIC17	chr20_63882783_G/C	Missense	<i>TPD52L2</i>	L27	QAGQKTSAAALSTLGSAIRKLGDMR
NIC17	chr3_136152028_C/A	Missense	<i>MSL2</i>	L28	VLRSLETVNTEFCCPNLQPNLEAT
NIC17	chr3_45500451_C/A	Missense	<i>LARS2</i>	L29	RYTDPHNPHSPFKTAVADYWMVPDL
NIC17	chr4_143538936_A/C	Missense	<i>SMARCA5</i>	L30	DSDWNPCQVQLQALDRAHRIGQTKTV

NIC17	chr4_76740029_C/A	Missense	<i>SHROOM3</i>	L31	QAQAWQAGEDKYSRSLPSEGDFQ
NIC17	chr6_31888379_C/T	Missense	<i>EHMT2</i>	L32	ARMVKHHCCPGCDYFCTAGTFLECH
NIC17	chr7_117791275_C/A	Missense	<i>CTTNBP2</i>	L33	SALATSQVGAWPSATPGLNQPACSD
NIC17	chr7_135209655_C/T	Missense	<i>WDR91</i>	L34	DYWSYLERLFLSHLEDIYRPTIHKL
NIC17	chr7_143291622_T/A	Missense	<i>CASP2</i>	L35	KKNRVVLAQQLMSELLEHILLEKDI
NIC17	chr7_4788195_C/A	Missense	<i>AP5Z1</i>	L36	APAASERPLWLDTYLRAPSCLEAFRD
NIC17	chr7_5715168_C/T	Missense	<i>RNF216</i>	L37	EQYQKDQQLIECHCCYGEFPFEELT
NIC17	chr7_756863_A/T	Missense	<i>DNAAF5</i>	L38	VFLKLILSTLKKSPSASGLLVLASA
NIC17	chr7_99035681_G/C	Missense	<i>SMURF1</i>	L39	ELIIGGLDKIDLKWDKSNTLKHCV
NIC17	chr9_131475787_G/A	Missense	<i>PRRC2B</i>	L40	RLSNCGYGRRTFISKEPHWQSXKSP
NIC17	chr9_72916962_G/C	Missense	<i>ALDH1A1</i>	L41	FVRRSVERAKYMLGNPLTPGVVTQG
NIC17	chr9_87706564_G/A	Missense	<i>DAPK1</i>	L42	CRWIHQGSTEGDTDIRLWVNGCKLA
NIC17	chrX_64921864_C/T	Frameshift	<i>ZC4H2</i>	L43	YKQEMDLLLQEKGPMWRNSD
NIC20	chr1_220157870_C/T	Missense	<i>RAB3GAP2</i>	L1	KSPKDRLCRRDVORMSDTAMTSFLGS
NIC20	chr12_25245351_C/G	Missense	<i>KRAS</i>	L2	MTEYKLVVVGARGVGKSAUTIQLIQ
NIC20	chr12_56324171_G/A	Missense	<i>PAN2</i>	L3	QAYRGAGGSFCSLGDSVIGQLFSC
NIC20	chr12_6529892_G/T	Missense	<i>NCAPD2</i>	L4	DNFDCFGDKLSDDSIIFASFLSVVGK
NIC20	chr12_6536969_G/A	Missense	<i>GAPDH</i>	L5	KIKWGDAGAEYVMESTGVFTTMEKA
NIC20	chr13_32339480_G/T	Missense	<i>BRC42</i>	L6	IFDGQPERINTAYVGNLYENNSN
NIC20	chr17_58511460_G/A	Missense	<i>MTMR4</i>	L7.1	IDSVESRDMFQLYISCKDSKVR
				L7.2	SVINVPLRMIDSVESRDMFQLYISC
				L7.3	RMIDSVERSRDMFQLYISCKDSKVR
NIC20	chr17_67911137_G/A	Missense	<i>BPTF</i>	L8	LEEKQRLEKIKLKGIGIGKGTSTN
NIC20	chr17_75960324_G/A	Missense	<i>ACOX1</i>	L9	GGLSLWIFTWCACPPCFTRQLRSS
NIC20	chr17_7673764_C/T	Missense	<i>TP53</i>	L10	VCACPGRDRRTEKENLRKKGEPHHE
NIC20	chr17_7673776_G/A	Missense	<i>TP53</i>	L11	FEVRVACPGRDWRTREEENLRKKGE
NIC20	chr18_80135747_G/A	Missense	<i>ADNP2</i>	L12	IDQELVIPCPCNIFASQPKVVGRHF
NIC20	chr19_46015404_C/A	Missense	<i>CCDC61</i>	L13	ERSLRARLKLTLRELALYKRGRRTP
NIC20	chr19_57254563_T/C	Missense	<i>ZNF805</i>	L14	TDVGRPFITSQTPVNIQELLLGKNF
NIC20	chr21_46389211_A/G	Missense	<i>PCNT</i>	L15	GAGALSTAPALGETWSVALPELD
NIC20	chr2_191363763_A/C	Missense	<i>MYO1B</i>	L16.2	RNAMQIVGFMDHDAESVLAJAVA
NIC20	chr2_196995406_A/T	Missense	<i>ANKRD44</i>	L17.1	LLILDKIQDESLNNEKNNALQTPLH
				L17.2	KCALLLDKIQDESLNNEKNNALQT
NIC20	chr3_49911685_G/A	Missense	<i>MON1A</i>	L18	TEGDEEDATEAWCLHQKHVFVLSA
NIC20	chr4_141721984_G/T	Missense	<i>IL15</i>	L19	KTEANWVNVISDFKKIEDLIQSMHI
NIC20	chr4_89113177_G/A	Missense	<i>TIGD2</i>	L20	ANSSDPTSGVKHSKMSSTSYYEELD
NIC20	chr5_112838822_T/TGTTTATACTG	Frameshift	<i>APC</i>	L21	DEIKQSEQRQSRNQSTTYPFILCLY
NIC20	chr5_112839978_AAGAG/A	Frameshift	<i>APC</i>	L22	AQTKREVPKNKAPTAEKRVDSLKLQ
NIC20	chr5_176577513_G/A	Missense	<i>CDHR2</i>	L23	GSASVQVLVRVSTLVTDYERQTA
NIC20	chr6_144493316_TTGAG/T	Frameshift	<i>UTRN</i>	L24	DVIQTHLDKCMKLYKTLKSNLKWKL
NIC20	chr6_157672728_A/G	Missense	<i>ZDHHC14</i>	L25	MYGATQSQSDMCQDQCQISTKFVL
NIC20	chr7_102637557_C/T	Missense	<i>UPK3BL1</i>	L26	GPEEAEGSVRRTTHTFSTPAEGAS
NIC20	chr7_152176502_G/A	Frameshift	<i>KMT2C</i>	L27.1	NVTVVSRVNVHVFFSGCAGKPRAHSR
				L27.2	VSRVNVHVFFSGCAGKPRAHRSINS
NIC20	chr7_93101806_G/A	Missense	<i>SAMD9</i>	L28	LQPIGLTYQFSELYFLASLLFWPEN
NIC20	chr9_14307385_C/T	Missense	<i>NFIB</i>	L29	KHEKRMSKDEERTVKDELSEKPEI
NIC20	chrM_6909_G/A	Missense	<i>MT-CO1</i>	L30	LATLHGSNMWKWSTAVLWALGFIFL
NIC22	chr1_197159613_G/A	Missense	<i>ZBTB41</i>	L01	PVQMPDTPSDLVCHTTLPPSSHEI
NIC22	chr1_218302341_A/G	Missense	<i>RRP15</i>	L02	SEKDHFYSDDDAVEADSEGAEP
NIC22	chr1_99884678_C/A	Missense	<i>AGL</i>	L03	FKSGSLAVDNADTILKIPFASL
NIC22	chr10_118040557_C/G	Missense	<i>RAB11FIP2</i>	L04	FEDKQRRKTEWFLESQKGRKIRNR
NIC22	chr10_132405164_G/A	Missense	<i>PWWP2B</i>	L05	RELRKPEEPENGKPTAAATARRSKM
NIC22	chr11_59615387_C/T	Missense	<i>OSBP</i>	L06	GSGAGGSGSAREDWLFWWTNYIKGY
NIC22	chr11_68157926_GAA/G	Frameshift	<i>KMT5B</i>	L07	YTEGLHENGVCCSDPLSLGVSN
NIC22	chr13_53050008_C/T	Missense	<i>OLFM4</i>	L08	SCGHGGVVNISKLSVQLNWRF
NIC22	chr14_104945557_G/T	Missense	<i>AHNAK2</i>	L09	DGARLEGDLAELKDVTAKDSKFM
NIC22	chr14_95091301_T/A	Missense	<i>DICER1</i>	L10	KEEDIEVPKAMGVIFESLAGAIYMD
NIC22	chr16_3677504_G/A	Missense	<i>TRAP1</i>	L11	SAAPGSLGYQWLLDGSGVFEIAEAS
NIC22	chr16_47669255_C/G	Missense	<i>PHKB</i>	L12	TGAFGHEEEVICNPLSPRIVQNI
NIC22	chr16_71690689_G/A	Missense	<i>PHLPP2</i>	L13	IRFYGEKPCHMDCLDRILLSGIY
NIC22	chr17_63821516_G/A	Missense	<i>FTSJ3</i>	L14	QQQQKQQQLPQTPLSCLTEIMSP
NIC22	chr17_6525386_C/T	Missense	<i>PITPNM3</i>	L15	SQWNSNDLVEQIKTMGLDEHQGEG
NIC22	chr17_7674221_G/A	Missense	<i>TP53</i>	L16.1	YMCNSSCMGGMNWRPILTIITLED
				L16.2	EVGSDCTTIHYNYMCNNSCMGGMN
NIC22	chr19_14161578_G/A	Missense	<i>ADGRL1</i>	L17	SPPLSTTTARPMLTASPAA
NIC22	chr2_127584256_G/A	Missense	<i>MYO7B</i>	L18	NISWDYIHYTDNQPTLDDLA
NIC22	chr2_31377127_C/A	Missense	<i>XDH</i>	L19	KPM
NIC22	chr22_28694075_G/C	Missense	<i>CHEK2</i>	L20	DLVKLLVVDPKGRFTTEALRHPW
NIC22	chr3_52259737_C/T	Missense	<i>WDR82</i>	L21	GSFIRLIDAFKGMVMHTFGGYANSK
NIC22	chr4_1238321_G/C	Missense	<i>CTBP1</i>	L22.1	LNKGLPLGVRPMMNGPLHPRPLV
				L22.2	MSGVRPPMMNGPLHPRPLVALLDGR

NIC22	chr5_112839525_A/AG		Frameshift	<i>APC</i>	L22.3	MCRRRLSDGVPPMMNGPLHPRPLVA
NIC22	chr5_57249510_G/T		Missense	<i>GPBP1</i>	L23	EADSANTLQIAEIKEKSSIGQLKIL
NIC22	chr6_118829150_C/T		Missense	<i>MCM9</i>	L24	LTRMRTDKKSEFFKALKRDRVEEEH
NIC22	chr7_45104146_C/T		Missense	<i>TBRG4</i>	L25	DPQESVSVNIALSSPLLSPFDLILV
NIC22	chr9_23701494_C/T		Missense	<i>ELAVL2</i>	L26	TSGEVAHCAKSFTLLKWLSPLFEA
NIC22	chrM_11031_G/CA		Frameshift	<i>MT-ND4</i>	L27	GQKPPGATEPITIKFANNPSQKTNQ
					L28.1	RHLSSPELRSKKTLPLYTNLPTNL
					L28.2	LSRKTKTPLTYTNLPTNLNNYNIHSH
NIC22	chrM_15731_G/A		Missense	<i>MT-CYB</i>	L29	FRPLSQSLYWLTLADLLLTWIGGQ
NIC22	chrM_9715_G/A		Missense	<i>MT-CO3</i>	L30	QMIQALLITLILLYFTLLQQASEYF
NIC25	chr10_132777741_C/T		Missense	<i>INPP5A</i>	L01	QYMNTRCPAWCDCILMSPSAKELVL
NIC25	chr10_34470134_C/G		Missense	<i>PARD3</i>	L02	SRKNPTRWSTTAFLKQNTAGSPKT
NIC25	chr11_107433697_T/A		Missense	<i>CWF19L2</i>	L03	DGGLSLWRKSYLSMKEQAEKQSRSNF
NIC25	chr11_72014750_C/T		Missense	<i>NUMA1</i>	L04	QEKMAATSKVEAHLETLVRKAGEQQ
NIC25	chr12_131913767_C/T		Missense	<i>ULK1</i>	L05	SLMCSGSSLVASVGLESHGRTPSPS
NIC25	chr1_21847754_C/T		Missense	<i>HSPG2</i>	L06	VEGQTLDLNCVVTROPQAIIWTWYKR
NIC25	chr12_25245350_C/A		Missense	<i>KRAS</i>	L07	MTEYKLVVVGAVGVGKSAUTIQLIQ
NIC25	chr1_243191320_C/G		Missense	<i>CEP170</i>	L08	STIHEIPTKDPTSHITGAGHSFT
NIC25	chr12_56088072_C/T		Missense	<i>ERBB3</i>	L09	NDSGACVPRCPOSLVYNNKLTQLEP
NIC25	chr13_75286844_C/T		Missense	<i>TBC1D4</i>	L10	PADALVNCDELLKDLNCNPNNKAKI
NIC25	chr14_24338294_A/C		Missense	<i>RIPK3</i>	L11	NRKASTASDVYSVGILMWAVLAGRE
NIC25	chr16_75656305_GGAA/G		Inframe deletion	<i>TERF2IP</i>	L12.1	ETQPDEEEEEEEKVSKPEVGAIIKI
NIC25					L12.2	ETQPDEEEEEEEEVSKPEVSISSQS
NIC25	chr17_20205400_G/GT		Frameshift	<i>SPECC1</i>	L13	HRERAEQLSQENEKLMNLLQERVKE
NIC25	chr17_7673607_TGCTA/T		Splice	<i>TP53</i>	L14.1	PHHELPPGSTKRGKQAGQEAVEETK
NIC25					L14.2	KQAGQEAVEETKGAVMPQIHFYHLS
NIC25					L14.3	AVMPQIHFYHLSPLFTAQQHQLLS
NIC25					L14.4	QHQLLSPAKEYTTGWRIFHPDSPWA
NIC25					L14.5	PLFTAQQHQQLLSPAKEYTTGWRIFH
NIC25	chr19_35738445_G/A		Missense	<i>IGFLR1</i>	L15	EGQKHIVIFALRHILRGEELTYDYK
NIC25	chr19_4524976_C/T		Missense	<i>PLIN5</i>	L16	LWGEWGQRPPEHRSRQAELETQLV
NIC25	chr19_46778729_C/T		Missense	<i>SLC1A5</i>	L17	LIYLFTRKNPYHFLWGIVTPLATA
NIC25	chr20_38156089_C/T		Missense	<i>TGM2</i>	L18	ASVDSLTFSVVTDPAPSQEAGTKAR
NIC25	chr20_41484523_C/T		Missense	<i>CHD6</i>	L19	KDDVEKNLAPKQKTIIEVELTNIQK
NIC25	chr20_50891831_A/C		Missense	<i>ADNP</i>	L20	MHNASDSEVDQDEVVEWKDGASPSE
NIC25	chr20_63930879_C/T		Missense	<i>DNAJC5</i>	L21	WAKALFVFCGLLMCCYCCCCCLCCCF
NIC25	chr2_230467207_G/T		Missense	<i>SP100</i>	L22	AEASSGALRSKHVEKAPMTSRSTST
NIC25	chr22_35334417_C/T		Missense	<i>TOM1</i>	L23	RLEDEFDMFALTGWGSSLADQRKEVK
NIC25	chr22_40266865_T/TC		Frameshift	<i>TNRC6B</i>	L24	SSGPQPATPKDEEPSGWEEPSPTVN
NIC25	chr2_86478667_A/G		Missense	<i>KDM3A</i>	L25	VHSVRAKWGIKADCPCSNSRQFKLFS
NIC25	chr3_24146684_C/T		Missense	<i>THR8</i>	L26.1	ECRFKKCIYVGMTTDLVDDSKRLA
NIC25					L26.2	QECRFKKCIYVGMTTDCHTFIKKWP
NIC25	chr4_147654416_C/T		Missense	<i>PRMT9</i>	L27	KSFTQNKDLSLENEAELCSALANL
NIC25	chr4_733979_G/T		Missense	<i>PCGF3</i>	L28.1	SEKSFHAKGPVGVVRADEASLRRAK
NIC25					L28.2	QKSHTLKVWLWVLSSEQMRPRLGERN
NIC25	chr4_8607369_G/A		Missense	<i>CPZ</i>	L29	LHGGDLVVSYPFNFSKHPQEEKMF
NIC25	chr5_112840204_CAG/C		Frameshift	<i>APC</i>	L30	QKDVELRIMPPVQENDNGNETIRAA
NIC25	chr5_136063199_A/G		Missense	<i>TGFBI</i>	L31	ELADSALEIFKQASAFSRPLSIRSY
NIC25	chr5_141384779_G/A		Missense	<i>PCDHGA2</i>	L32	GLFAVGLYTGEVHTARALLRDALK
NIC25	chr5_180948367_C/T		Missense	<i>BTNL8</i>	L33	KIFFSKFQWKIQLVQELDWRKHGQAE
NIC25	chr6_139166833_C/CACCGGGCTA		Inframe insertion	<i>HECA</i>	L34.1	GGSPGQSPPTGTYGYSILSPAHFSG
NIC25					L34.2	GSPGQSPPTGTYGYSILSPAHFSGP
NIC25					L34.3	SPGQSPPTGTYGYSILSPAHFSGPR
NIC25	chr7_158167215_C/T		Missense	<i>PTPRN2</i>	L35	AHTSALTYPPGSQTLRDLPLPRTL
NIC25	chr8_126556693_G/T		Missense	<i>FAM84B</i>	L36	LRIGKQPYRLQIKLQAQRSHTLEFQ
NIC25	chr9_83970226_G/A		Missense	<i>HNRNPK</i>	L37	IKIDEPLEGSEDWIITITGTQDQIQ
NIC25	chrX_71250094_G/A		Missense	<i>ZMYM3</i>	L38	SVCLSLYEQQQCPIPQSGDPADAT
NIC27	chr10_87170897_A/T		Missense	<i>SHLD2</i>	L1	GQKQKKVMLTVELAQDQHYALVLWG
NIC27	chr1_114716126_C/T		Missense	<i>CSDE1</i>	L2	MTEYKLVVVGADGVGKSAUTIQLIQ
NIC27	chr11_46778488_C/T		Missense	<i>CKAP5</i>	L3	DGDEPDGDSNDVIDLPRTEISDKI
NIC27	chr1_202012640_A/AC		Frameshift	<i>ELF3</i>	L4.1	AFQEALDPGPFDPGQPLCPGAAGRR
					L4.2	PGQPLCPGAAGRRSASQPLPRLPQ
					L4.3	AGRRSASQPLPRLPQWRRSPLPWQ
NIC27	chr1_237658004_C/A		Missense	<i>RYR2</i>	L5	EYFINKYAEHSHEKWSMDKLANGWI
NIC27	chr14_45006152_G/A		Missense	<i>KLHL28</i>	L6	RGISLLPDKAIDLNTVGHKKKEPDD
NIC27	chr16_12069072_G/T		Missense	<i>SNX29</i>	L7	VGSYSPADAPLGILENGTGPEDHVL
NIC27	chr16_3138989_G/T		Missense	<i>ZNF213</i>	L8.1	TCFVSGVHGPVAFGDIPIFYFSREEW
NIC27	chr16_3138989_G/T		Missense	<i>ZNF213</i>	L8.2	QEQQHSHSGTCGIWRHPIFLPGRMG
NIC27	chr19_3738627_G/A		Missense	<i>TJP3</i>	L9	EAVQFLGLPPIGKEMELVTQRKQDI
NIC27	chr19_49867076_G/T		Missense	<i>PNKP</i>	L10.1	LVLGRGPLTQVTERKCSRTQVELVA
					L10.2	DGQALVLGRGPLTQVTERKCSRTQA

NIC27	chr20_63590574_C/T	Missense	GMEB2	L11	RPRRLARATSGPATMASQVLTQSAQL
NIC27	chr2_170846011_G/T	Missense	GAD1	L12	TDNVILIKCNERVKUIPADFEAKIL
NIC27	chr3_15074555_G/A	Missense	RBSN	L13	DLQREQLQMLREWELEEREREQFRVA
NIC27	chr3_151199322_T/TA	Frameshift	MED12L	L14.1	VYKDLEPTFYFFLSFPCWNWYWKLF
				L14.2	FSFPCWNWYWKFCNLGFYTEEYESQ
				L14.3	YWKLCNLGFYTEEYESQVCEHLLN
NIC27	chr3_97877501_G/A	Missense	CRYBG3	L15	DDSSQEDILSSEISPGHHGPRKSRD
NIC27	chr4_17501822_GCT/G	Frameshift	QDPR	L16.1	SLFKNCCLMWKQHMDIDHLQKGCPG
				L16.2	MDIDHLQKGCPGWDWSYDRVRHGQG
				L16.3	WDSWYDRVRHGQGCCPALPEPGWE
				L16.4	GCCSPALPEPGWEEQRHAARGSRHR
				L16.5	EQRHAARGSRHRCAPGYPGYPDEQE
				L16.6	HAARGSRHRCAPGYPGYPDEQEINA
				L16.7	SLFKNCCLMWKQHMDIDHLQPSGYQ
				L16.8	MDIDHLQPSGYQASQGRPPDLGWR
				L16.9	ASQGRRPPDLGWRKGCPGWDWSVTL
				L16.10	RRPPDLGWRKGCPGWDWSVTLDTPM
NIC27	chr4_17813010_G/A	Missense	NCAPG	L17	LLGSMPPENAQIDNDVFDKINKAMLI
NIC27	chr4_8235554_G/A	Missense	SH3TC1	L18	GAWEREKAVSFYQDRALPLAVTTGN
NIC27	chr4_9890687_G/A	Missense	SLC2A9	L19	AVFSGLVIEHLGWRPLIGGFLMG
NIC27	chr5_150204571_G/A	Missense	SLC6A7	L20	GMYWLVLDDYSTSFGLMVVITTC
NIC27	chr6_33711605_C/A	Missense	UQC2C	L21	WPVDETKRGRDLCAYLQRQAQAFR
NIC27	chr7_98984093_C/T	Missense	TRRAP	L22.1	SSIFMWRQHHYQIVTAYENSSQHD
				L22.2	QGKPTWSGMHSSLIVTAYENSSQHD
NIC27	chr8_144057495_G/T	Missense	OPLAH	L23	PLSLEEVAMGFVSVANEAMCRPIRA
NIC27	chr8_144360298_A/G	Missense	FBXL6	L24	AAGTPGPDPKACQLLARSACLLG
NIC27	chr8_28160331_C/T	Missense	ELP3	L25	PDQDILIGLLRLCKCSEETFRFELG
NIC27	chr8_39918906_C/A	Missense	IDO1	L26.1	LPPILVYADCYLENWKKDPNKYVN
				L26.2	LPPILVYADCYLENWKKDPNKPLT
NIC38	chr1_114713909_G/T	Missense	NRAS	L01	ETCLLDILDTAGKEEYSAMRDQYMR
NIC38	chr1_155187338_G/C	Missense	MUC1	L02.1	AVCQCRRKNYGQVDIFPARPTYHPM
				L02.2	GCLSVPPKELRAGGHLSSPGYPILSY
				L02.3	WLSVSAEARTTGRWTSFQPGIPTIL
NIC38	chr1_204968350_G/A	Missense	NFASC	L03	VLRGMDDLCEITSGVPTPDIAYWK
NIC38	chr1_52359809_G/A	Missense	CC2D1B	L04	SAQPVSDDLDPDWALLSSRQREYKV
NIC38	chr10_127439193_C/A	Missense	DOCK1	L05	FEKEFKPTDISLKQSEAVILSETIS
NIC38	chr10_87790413_T/C	Missense	ATAD1	L06	VDPLNMHVTVSDMAGLDDVITDLKD
NIC38	chr11_114407658_C/T	Missense	RBM7	L07	PYLA DRHYSREQCYTDHGSDDHYRG
NIC38	chr11_68934473_G/A	Missense	IGHMBP2	L08	EDEQS KGNPGEVHVLSLHIQALVDA
NIC38	chr11_75796404_G/A	Missense	DGAT2	L09	IFGYHPHIGMLDAFCNFSTATEEV
NIC38	chr12_100623662_C/T	Missense	GAS2L3	L10	LLKYDPCRILQFVTLEQKILAFQKG
NIC38	chr12_25245347_C/T	Missense	KRAS	L11	MTEYKLVVGAGDVGKSAUTIQLIQ
NIC38	chr12_50474099_C/T	Missense	LARP4	L12.1	TTIPVSPPTTKSSRASTASP CNNN
NIC38	chr12_50474099_C/T	Missense	LARP4	L12.2	TTIPVSPPTTKSSREPRKLYSAEV
NIC38	chr12_57268355_C/T	Missense	R3HDM2	L13	VSQSVQGGGLPAARVPVYMSIMPPAQ
NIC38	chr12_6974548_TCA/T	Splice	EMG1	L14.1	NGRDPGEARPDITHQVTPGTVLTTL
				L14.2	DPEGEARPDITHQVYIHTQKNVLE
				L14.3	YIHTQKNVLEVNQPQTRIPRTFDRF
				L14.4	PQTRIPRTFDRFCGLMVQLLHKL SV
				L14.5	GLMVQLLHKL SVRAADGPQKLKVI
				L14.6	ILLKNGRDPGEARPDITHQFADADG
NIC38	chr13_24883229_C/T	Missense	CENPJ	L15	ANGHQETK YRSQIRVKDKEGNVLM
NIC38	chr14_64948446_G/A	Missense	RAB15	L16	QAHRKELEG LRM CASNELA ELEE
NIC38	chr16_2117882_G/T	Missense	PKD1	L17	ALELVCPSVQSEE LDSLQNSQRG C
NIC38	chr17_42670596_C/T	Missense	PLEKHH3	L18	PLHPEGLSPDGKHLPFLFEOQAHALL
NIC38	chr17_47292436_G/A	Missense	ITGB3	L19	QQDECSPREGQPICSQRGECLCGQC
NIC38	chr17_72124031_TC/T	Frameshift	SOX9	L20	PQAHTLTTLSSEPGQSSERTSRRSS
NIC38	chr17_7674229_C/A	Missense	TP53	L21.1	HYN YM CNSSCMGV MNRRPILT I
				L21.2	EVGSDCTTIIHYN YM CNSSCMGV MNRRPILT
NIC38	chr17_81811574_G/A	Missense	GCGR	L22	VSTWLS DGVSPP QRPQAGGWVG SQA
NIC38	chr18_25226861_A/T	Missense	ZNF521	L23	SNSPSLTVG YTTV S TTPDSN LSV
NIC38	chr18_50275897_C/T	Missense	MBD1	L24	GAC STCLLQPLHN VAS GLF CKCERR
NIC38	chr19_3981442_G/A	Missense	EEF2	L25	QLIDP IFKV FDVIM NF KKE TAKL
NIC38	chr19_44288724_G/T	Missense	ZNF235	L26	DDNIVH KRD KV H RNS DC G KDTL KV S
NIC38	chr19_49168357_G/GT	Frameshift	TRPM4	L27.1	RDHQM ASTGGT KWW PWW PPGV WS
				L27.2	WW PWW PPGV WS G ITPS ST PRARS
				L27.3	IETPS ST PRARS LRG TGG AVTR RTG
				L27.4	RGT GAV TR RTG SSFP WTTTRPSS
				L27.5	SFP WTTTRPSS WW TTA HTAA WGA R
				L27.6	WTTA HTAA WGA RTA SACAW SPT SHS
				L27.7	ASACAW SPT SHS RRA WEGLE LTL S

NIC38	chr19_49909636_C/T	Missense	<i>NUP62</i>	L28	AWSPTSHSRRRAWEGLELTSLCSS
NIC38	chr19_54192199_A/G	Missense	<i>TSEN34</i>	L29	GPSDGQHWGHQGVVAMGVAPWGVVVR
NIC38	chr2_132785077_C/A	Missense	<i>NCKAP5</i>	L30	L27.10 PSDGQHWGHQGVVAMGVAPWGVVVRN
NIC38	chr2_218740117_T/C	Missense	<i>TTLL4</i>	L31	L27.11 GTIRWPALGAPRCGGHHGCGPLGCGP
NIC38	chr2_25243924_A/T	Missense	<i>DNMT3A</i>	L32	L27.12 TIRWPALGAPRCGGHHGCGPLGCGPE
NIC38	chr2_54850185_G/A	Missense	<i>EML6</i>	L33	WSDLSKYLTQNTDSAGERLFYRMPMSG
NIC38	chr2_70088042_T/G	Missense	<i>PCBP1</i>	L34	TNSTAASRPPVTRRLVVPATQCGSL
NIC38	chr20_25207212_G/A	Missense	<i>ENTPD6</i>	L35	GVFIYVAYIKWHQATAQAFFSITR
NIC38	chr20_38558332_C/T	Missense	<i>RALGAPB</i>	L36	EPANSRLPPLHILVLDSTIPGFFDDI
NIC38	chr20_58909366_G/A	Missense	<i>GNAS</i>	L37	DYVPSDQDLLRCHVLTSIFETKFKQ
NIC38	chr22_41176347_G/A	Missense	<i>EP300</i>	L38	PDPLIPCDLMDGQDAFLTLARDKHL
NIC38	chr22_41604044_C/T	Missense	<i>DESI1</i>	L39	LEYLSSLGESLFQGEAYNLFEHNCR
NIC38	chr3_50276335_C/T	Missense	<i>SEMA3B</i>	L40	QVLAEERTERTAWGLLLRLLRRRDS
NIC38	chr3_77577541_A/G	Missense	<i>ROBO2</i>	L41	PQSVTVLTGSYSSSTSISVSWDPPP
NIC38	chr4_75969346_C/T	Missense	<i>SDAD1</i>	L42	LKQLECCKERFEMKMMMLMNLISRLV
NIC38	chr5_112839514_TAAAAG/T	Frameshift	<i>APC</i>	L43	IGCNQTQQEADSANTLQIAEKDWN
NIC38	chr5_140835112_C/A	Missense	<i>PCDH47</i>	L44	TVDNNNDNAPVFERTLYTVKLPENV
NIC38	chr5_14610204_T/A	Missense	<i>OTULINL</i>	L45	LEVLIKVFRFLFKINSRDFEVYPEE
NIC38	chr7_100684319_G/A	Missense	<i>GIGYF1</i>	L46	SPPPLLGNMDQEWLKKQQELAAAAL
NIC38	chr7_1496228_C/T	Missense	<i>INTS1</i>	L47	ERFVVHITDVLAMSSMMLGITAQVKE
NIC38	chr7_155803327_C/T	Missense	<i>SHH</i>	L48	VRPGQRVVVAEHDGDRRLPAAVH
NIC38	chr7_5388319_G/A	Missense	<i>TNRC18</i>	L49	AAKLFGLEPGRPLPTGPEHKWPFE
NIC38	chr7_98229051_C/T	Missense	<i>TECPRI</i>	L50	HTAWVYTGGYGGSCFGQGLASSTSNI
NIC38	chr8_121617152_C/G	Missense	<i>HAS2</i>	L51	MLDPASSVEMVKLLEEDPMVGVGVGG
NIC38	chr9_106925857_C/T	Missense	<i>ZNF462</i>	L52	SSLPLENETDSHSSSSNTVKKSQTS
NIC38	chr9_93289156_G/A	Missense	<i>WNK2</i>	L53	CTPAPEAASTRDTSATPREPLPAPP
NIC38	chr1_203347520_T/TGTACAGCTG	Inframe insertion	<i>FMOD</i>	L54.1	PDGLPSALEQLYSCTMEHNINVYTP
NIC39	chr10_118039249_C/T	Missense	<i>RAB11FIP2</i>	L01	LPRKKNPFEESSKTWDSSMMNLFSKP
NIC39	chr11_19933968_A/G	Missense	<i>NAV2</i>	L02	GIPKPGMKSMMPGRSPSAPAPSKEGE
NIC39	chr1_144424696_C/T	Missense	<i>NBPF15</i>	L03	ALEEKHVGFSLDMGEIEKKKGKGR
NIC39	chr1_19186599_G/A	Missense	<i>UBR4</i>	L04	RKGSMSDDASASIDSNTYYEDDFSS
NIC39	chr11_93700058_C/A	Missense	<i>CEP295</i>	L05	QDNLNLQKQLDIQREVLHYSQKAQ
NIC39	chr1_202013255_CAA/C	Frameshift	<i>ELF3</i>	L06.1	GKRKRGRPRKLSRVLGLSRGQEEQA
				L06.2	VGLSLRGQEEQARAQRHPPVGVHPG
				L06.3	AQRHPPVGVHPGPHPPGAQRGPHEVGESA
				L06.4	PVGVHPGPHPPGAQRGPHEVGESA
NIC39	chr12_121453254_G/A	Missense	<i>KDM2B</i>	L07	LAANRTTAGARRCRTRCRICEACLR
NIC39	chr12_25245350_C/A	Missense	<i>KRAS</i>	L08	MTEYKLVVVGAVGVGKSAUTIQLIQ
NIC39	chr12_58879049_C/T	Missense	<i>LRIG3</i>	L09	TPMDLTIRAGAMTRLECAAVGHPAP
NIC39	chr13_19659265_T/A	Missense	<i>MPHOSPH8</i>	L10	GDYITVKVALNSKEEYNLDQEDSSG
NIC39	chr14_104171738_C/T	Missense	<i>KIF26A</i>	L11	NPGSIGKVKVMLWIWPAQGAQRSAE
NIC39	chr14_22902052_C/CGGT	Inframe insertion	<i>RBM23</i>	L12	QLPSTAAAAAAAPAAQAAALQLNGA
NIC39	chr1_46272733_G/A	Missense	<i>RAD54L</i>	L13	YKRFLRQAKPAEKLLEGKMSVSSL
NIC39	chr14_88792343_T/C	Missense	<i>EML5</i>	L14	GVGVVYSPREHRRKFYRGHSDDIIIS
NIC39	chr15_34982598_C/A	Missense	<i>ZNF770</i>	L15	QGGFENGIEGESDENNPFLDVHSIYI
NIC39	chr16_22534398_C/T	Missense	<i>NP1PB5</i>	L16	PLPPSADDNLKTLSERQLTPLPPSA
NIC39	chr16_549404_C/T	Missense	<i>CAPN15</i>	L17	EGAYQVRLCKDGMWTTVLVWDDMLPC
NIC39	chr16_58267555_A/G	Missense	<i>CCDC113</i>	L18	DKEILLRKELLERIEKETLQVEEDR
NIC39	chr16_90006391_G/A	Missense	<i>DBND1</i>	L19	QSHEKQPLGDPEWQATVLDTFLTVE
NIC39	chr17_47292436_G/A	Missense	<i>ITGB3</i>	L20	QQDECSPREGQPICSRQGECLCGQC
NIC39	chr17_51041572_C/T	Missense	<i>SPAG9</i>	L21	GDGLLTPDAQKGRETGPSEQWKFQE
NIC39	chr17_7675088_C/T	Missense	<i>TP53</i>	L22	YKQSQHMTEVVRHCPHHERCSDSDG
NIC39	chr19_19202339_ATGTT/A	Inframe deletion	<i>RFXANK</i>	L23.1	LHKIVDFYPEDNSLQTFPIPAAEVD
				L23.2	LHKIVDFYPEDNSLQICSCPFCWGGW
NIC39	chr19_3193350_G/C	Missense	<i>NCLN</i>	L24	AMETAVPVYFAVQDEALLSIYKQTQ
NIC39	chr19_41116275_G/T	Missense	<i>CYP2F1</i>	L25	CLLTLSSRDKGNLPPGPRPLSILG
NIC39	chr19_6534932_C/T	Missense	<i>TNFSF9</i>	L26	FQGRLLHLSAGQCLGVHLHTEARAR
NIC39	chr19_9980686_C/G	Missense	<i>COL5A3</i>	L27	PGATGQPGPKGDLGQDGAPGIPGEK
NIC39	chr20_5922477_C/A	Missense	<i>CHGB</i>	L28	SSRGEAGAPGEEEIQGPTKADTEKW
NIC39	chr2_131052950_G/A	Missense	<i>FAM168B</i>	L29	PVAPHVPTVPTYWAPGPTPTSYVPP
NIC39	chr21_46389270_G/C	Missense	<i>PCNT</i>	L30	LPELDRTLSECAQMSSVAEISSHMR
NIC39	chr2_24024246_G/A	Missense	<i>MFSD2B</i>	L31.1	MVGSTPKTPSRDTSSRSLRRTSY
				L31.2	LCILMVGSTPKTPSRDTSSRSLRRLR
				L31.3	MVGSTPKTPSRDTSSRSLRRLVHH
NIC39	chr22_41177044_G/C	Missense	<i>EP300</i>	L32	QHTKGCKRKTNGACPICKQLIALCC
NIC39	chr3_129250763_C/T	Missense	<i>COPG1</i>	L33	SAVLQEASDICSPALIFIINIHQCQ

NIC39	chr3_133838231_G/A	Missense	<i>RAB6B</i>	L34	DKRQITIEEGEQCAKELSVMFETS
NIC39	chr3_64615973_G/A	Missense	<i>ADAMTS9</i>	L35	CSGECNTGGWRYFAWTECSKSCDGG
NIC39	chr4_883459_C/T	Missense	<i>GAK</i>	L36	LDISVITSRIAVISFPAEGVESALK
NIC39	chr4_989975_C/T	Missense	<i>IDUA</i>	L37	QLHKRGSSVAGNIPTGFMPQVPE
NIC39	chr5_112839783_GA/G	Frameshift	<i>APC</i>	L38.1	SRCTSVSSLDSFGVVRLPAPFRVNH
				L38.2	SVSSLDSFGVVRLPAPFRVNHAVEW
NIC39	chr5_1338974_G/GCACT	Frameshift	<i>CLPTM1L</i>	L39	INLLTGESDTQQIEAEKKPTSECPG
NIC39	chr5_141955118_G/A	Missense	<i>RNF14</i>	L40	PQRPPASSATLRWQRHLNGKVSPK
NIC39	chr6_106511835_G/A	Missense	<i>CRYBG1</i>	L41	HENDSPQLEPLETEGEFPFDATTTA
NIC39	chr6_119348513_G/A	Missense	<i>MAN1A1</i>	L42	PVDFVPIIGVESWEPADAIREKRA
NIC39	chr6_1312718_T/C	Missense	<i>FOXQ1</i>	L43	MKLEAFVPRAAHGDKQGSDELEGAGG
NIC39	chr6_149378140_G/C	Missense	<i>TAB2</i>	L44	SDDSGISGLRNHITSLNLDLQSQNI
NIC39	chr6_38703045_G/A	Missense	<i>GLO1</i>	L45	MAESQPSSGGLTDEAALSCSDADP
NIC39	chr6_4130838_TG/T	Frameshift	<i>C6orf201</i>	L46	KLKLYALYKQATEGPCNMNPQNQVLT
NIC39	chr7_134661775_C/T	Missense	<i>BPGM</i>	L47	WVPVESSWRNLNECHY GALIGLNREQ
NIC39	chr7_144363086_T/G	Missense	<i>ARHGEF5</i>	L48	CPIQSEHLDMAPLSSDLGSEEEVE
NIC39	chr7_43624714_G/C	Missense	<i>COA1</i>	L49	TKESIVTEELIVLTSYTLGQCRCQSE
NIC39	chr8_39922577_C/T	Missense	<i>IDO1</i>	L50	LTYENMDVLFSCDCSKGFFLVS
NIC39	chr8_52657517_G/A	Missense	<i>RB1CC1</i>	L51	MMVESLYSSVINVIDSRRMQDTNVC
NIC39	chr9_106927814_G/T	Missense	<i>ZNF462</i>	L52	PALKATVTSIMRLAFLDGlieAGYH
NIC39	chr9_127482955_G/C	Missense	<i>LRSAM1</i>	L53	SEILKSLENERITMEQLMSITQEEET
NIC39	chr9_136854652_G/T	Missense	<i>PHPT1</i>	L54	AGGPERPSWPRRYHSRNSAQGSFLV
NIC39	chrM_5227_G/A	Missense	<i>MT-CO2</i>	L55	TPLIPSTLLSLGDPPLTGLPKWA
NIC39	chrX_53580849_G/C	Missense	<i>HUWE1</i>	L56	VANCCIRIALPAARGSGTASDDEF
NIC39	chrX_70287275_C/A	Splice	<i>KIF4A</i>	L57.1	NDVDFQDIEHSKIIIAKKRGLCTR
				L57.2	IIIakkRGLCTRKLQPTALHVDSVM
				L57.3	IAKKRGLCTRKLQPTALHVDSVMTC

SLP - synthetic long peptide

Table S3 | 40-marker imaging mass cytometry panel

Target	Clone	Metal	Incubation Time	Temp	Dilution
B catenin	D10A8	89Y	Overnight	4C	100
TGFbeta	TB21	115In	5h	RT	100
HLA-DR	TAL 1B5	141 Pr	5h	RT	100
CD20	H1	142 Nd	Overnight	4C	100
CD68	D4B9C	143 Nd	Overnight	4C	100
CD11b	D6X1N	144 Nd	5h	RT	100
CD4 +2nd Ab	EPR6855	145 Nd	Indirect ON	RT	100
CD8a	D8A8Y	146 Nd	5h	RT	50
CD31	89C2	147 Sm	Overnight	4C	100
TCRgd + 2nd Ab	H41	148 Nd	Indirect ON	4C	50
CD45	D9M8I	149 Sm	Overnight	4C	50
Granzyme B	D6E9W	150 Nd	5h	RT	100
CD57	HNK-1 / Leu-7	151 Eu	Overnight	4C	100
Ki-67	8D5	152 Sm	Overnight	4C	100
CD3	EP449E	153 Eu	Overnight	4C	50
TIM3	D5D5R	154 Sm	5h	RT	100
LAG-3	D2G40	155 Gd	5h	RT	50
PD-L1	E1L3N	156 Gd	Overnight	4C	50
CD39	EPR20627	157 Gd	5h	RT	100
VISTA	D1L2G	158 Gd	5h	RT	100
FOXP3	D608R	159 Tb	Overnight	4C	50
PD-1	D4W2J	160 Gd	5h	RT	50
ICOS	D1K2T	161 Dy	5h	RT	50
IDO	D5J4E	162 Dy	Overnight	4C	100
CD14	D7A2T	163 Dy	5h	RT	100
CD204	J5HTR3	164 Dy	5h	RT	50
CD45RO	UCHL1	165 Ho	Overnight	4C	100
PDPN	D2-40	166 Er	Overnight	4C	100
CD56	E7X9M	167 Er	5h	RT	100
CD103	EPR4166(2)	168 Er	5h	RT	50
CD38	EPR4106	169 Tm	Overnight	4C	100
Tbet	4B10	170 Er	5h	RT	50
CD15	MC480	171 Yb	Overnight	4C	100
Cleaved-caspase	5A1E	172 Yb	5h	RT	100
CD163	D6U1J	173 Yb	5h	RT	50
CD7	EPR4242	174 Yb	5h	RT	100
p16ink4a	D3W8G	175 Lu	Overnight	4C	100
CD11c	EP1347Y	176 Yb	5h	RT	100
Vimentin	D21H3	194 Pt	Overnight	4C	50
Keratin	C11 and AE1/AE3	198 Pt	Overnight	4C	50

Table S4 | Number of T cells at sorting and after expansion.

Patient	#Cells				% Cells				Primary expansion rate				Restimulation expansion rate			
	DP	SP	DN	SP39	DP	SP	DN	SP39	DP	SP	DN	SP39	DP	SP	DN	SP39
NIC4	610	1447	1792	353	11,7	37,6	47,3	3,42	157377	32480	42410					
NIC5	595	51	185	94	61	7,32	24,1	7,89	882352	145945						
NIC7	1110	738	3549	246	25,0	13,9	52,1	9,0	2703		10989					
NIC16	8342	301	445	84	91,0	3,3	4,4	1,4	4075			16809				
NIC17	2095	727	2677	24	38,6	15,9	44,8	0,7				207317				
NIC20	287	418	650	29	29,6	28,6	37,5	4,3	142857	74163	63077		5980	4270		
NIC22	31000	649	484	51	96,5	2,0	1,3	0,2	7419	37750	32231					
NIC25	224	895	478	18	23,2	50,6	23,5	2,7		2123	17364		232143			
NIC27	6574	1602	2070	95	66,5	14,2	16,5	2,8	11409	8115	26962					
NIC38	29768	157	409	NA	97,4	0,7	1,6	0,3	2284	40764	18582					
NIC39	1400	5337	1821	136	26,6	52,7	18,7	2,1		2248	4723					

SP - CD103+CD39-